# Constraining Neutron-Star Matter with Microscopic and Macroscopic Collisions

Huth, Pang et al. Nature 606 (2022) 276-280
Pang et al arxiv:2205:08513

Peter T. H. Pang

Nikhef

Utrecht University

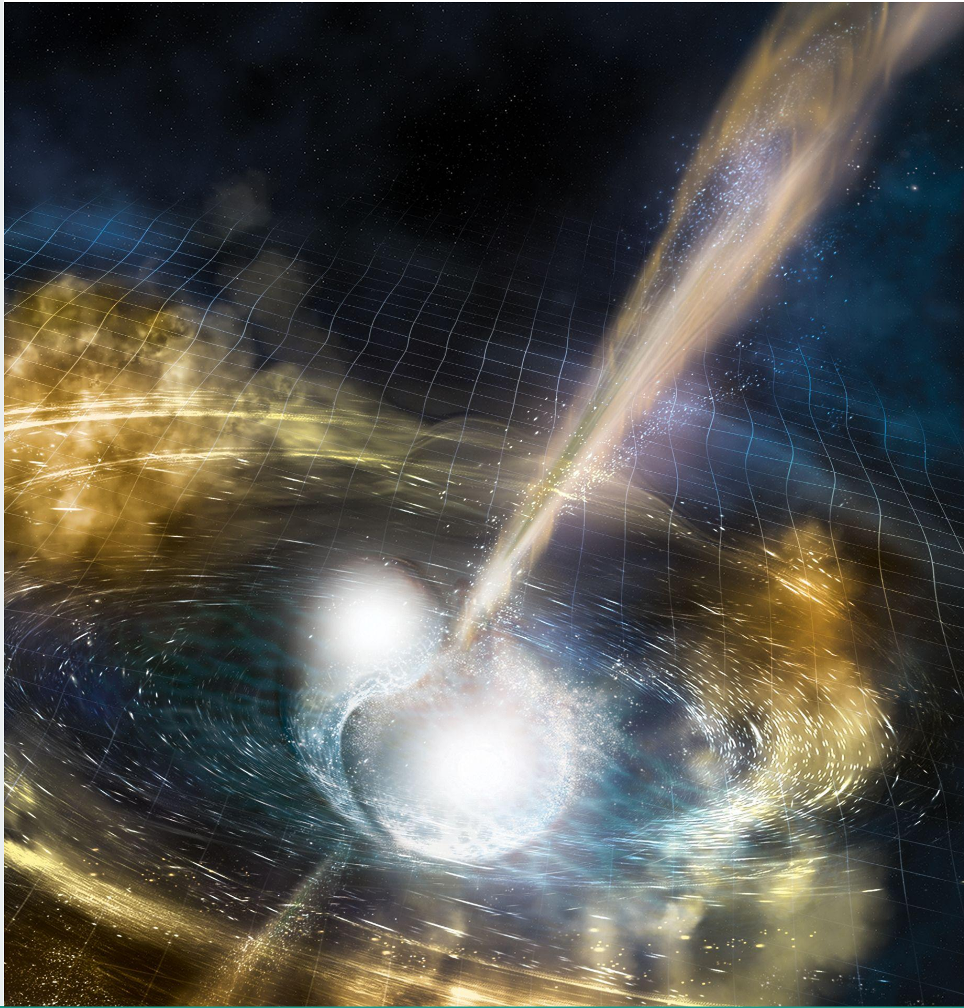

Credit: National Science Foundation/LIGO/Sonoma State University/A. Simonnet

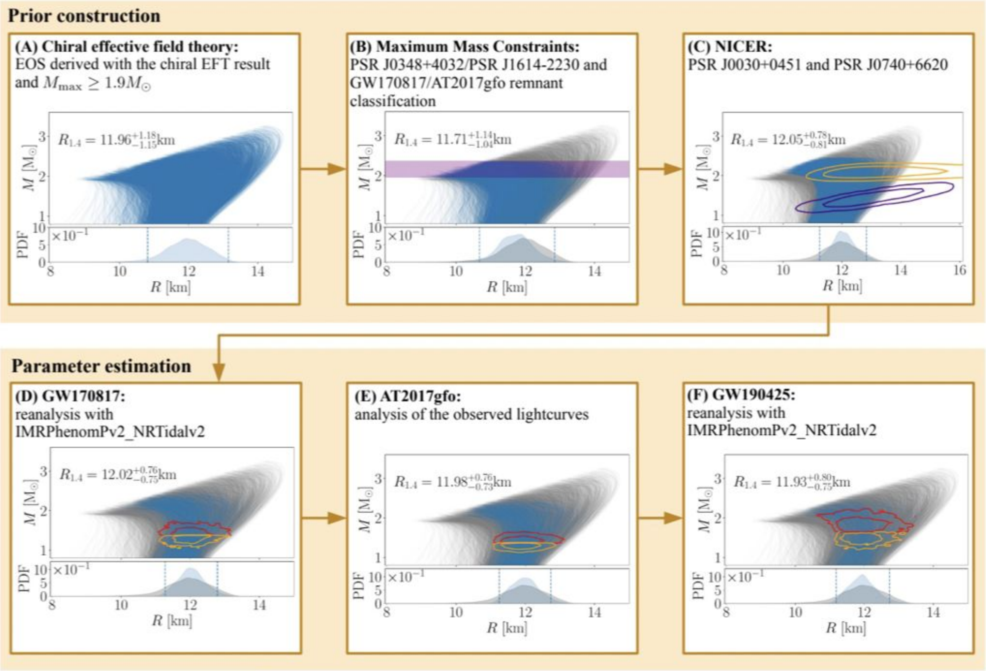


**Combining**

- chiral effective field theory
- radio pulsar measurements
- X-ray NICER measurements
- gravitational waves
- kilonova observations
- HIC

TD et al. Science, Vol. 370, Issue 6523, pp. 1450-1453
Huth et al., Nature 606 (2022) 276-280

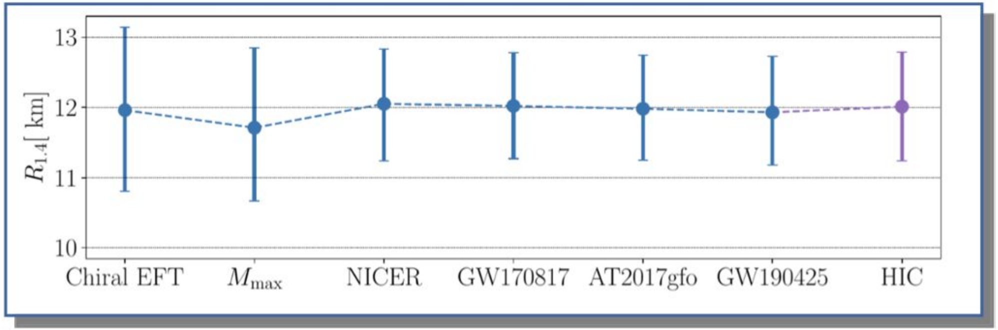


NMMA

cf. talk by Peter Pang


Observations / Experiments
Theory / Model
Bayesian machinery
Physics

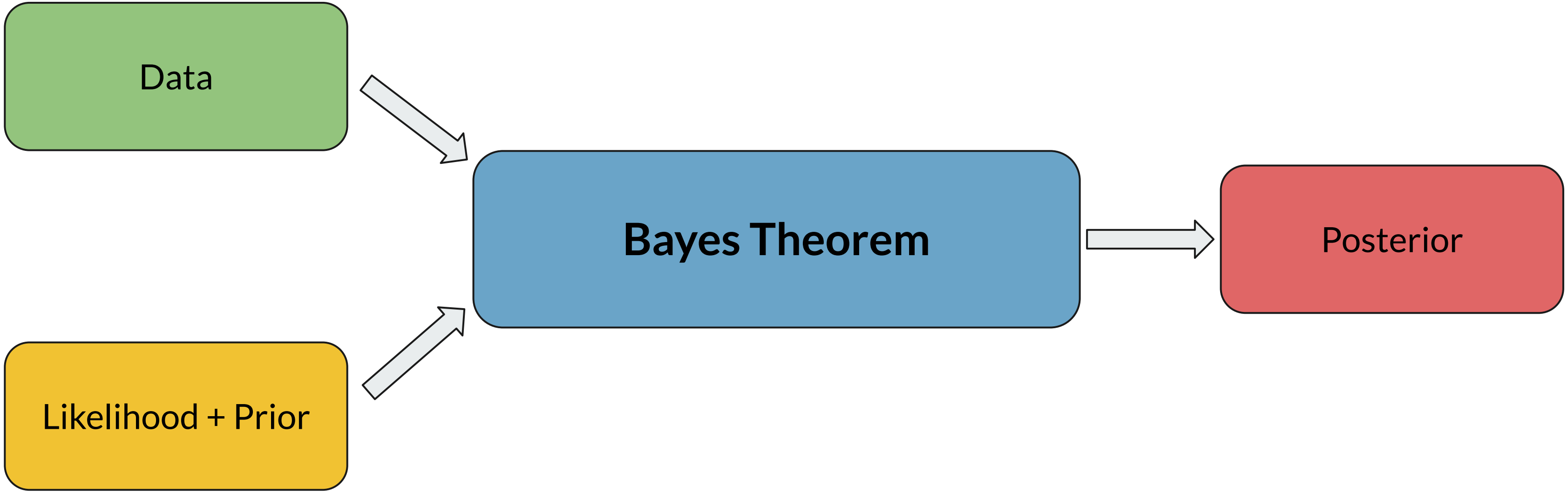
Data
Likelihood + Prior
Bayes Theorem
Posterior

# Prior on the EOS

- Chiral effective theory below 1.5 nsat
- Speed-of-sound extrapolation (CSE) afterwards
- EOS with first-order phase transitions (i.e., segment with cs = 0) are added

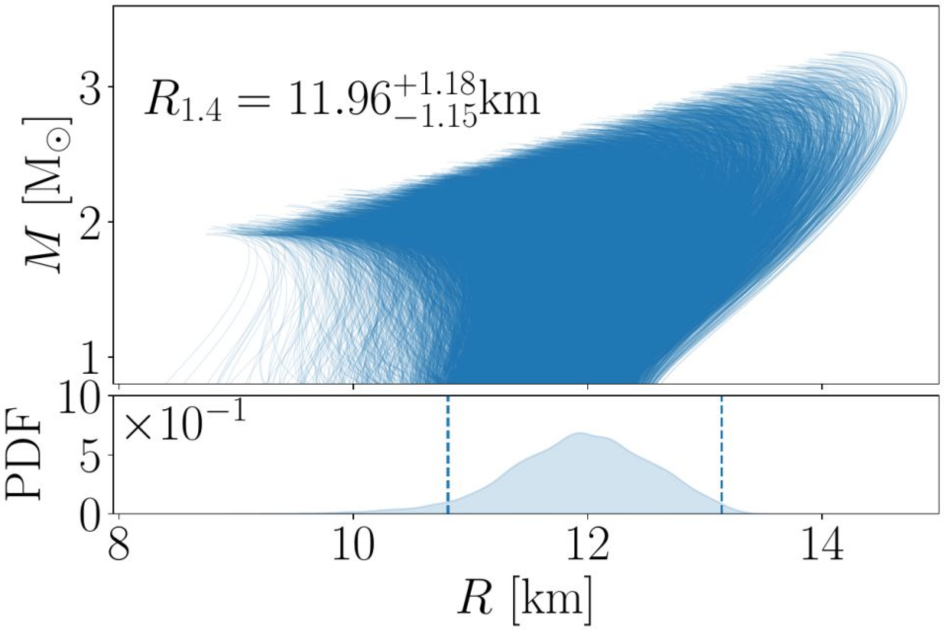

# Radio pulsars

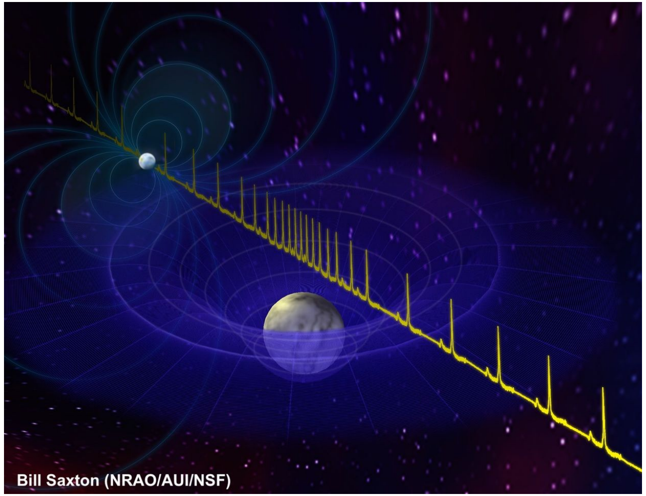


| Pulsar | Mass is $M_\odot$ |
|---|---|
| PSR J0348+4032 | $2.01 \pm 0.04$ |
| PSR J1614−2230 | $1.908 \pm 0.016$ |

$$\mathcal{L}_{\mathrm{PSR}}$$

$$= p(\mathrm{PSR}|\mathrm{EOS}) \propto \int_0^\infty p(m|\mathrm{PSR})p(m|\mathrm{EOS})$$

$$= \int_0^{M_{\mathrm{max}}} p(m|\mathrm{PSR});\ \ p(m|\mathrm{EOS}) = 1/M_{\mathrm{max}}(\mathrm{EOS})$$

# GW170817 reamant

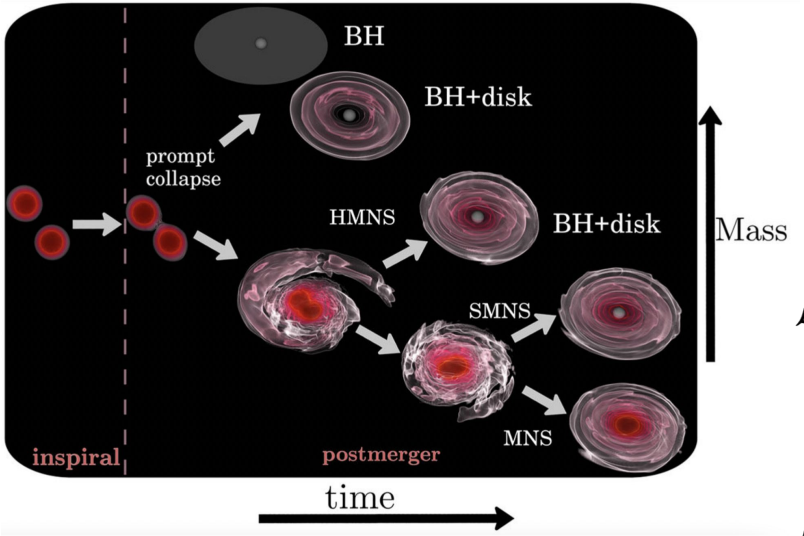


- GW170817 results in a black hole
- Numerical-relativity motivated fitting
- Upper bound on the maximum mass
- c.f. Rezzolla's talk on Tuesday

$$\mathcal{L}_{M_{\rm bound}} = p(M_{\rm bound}|{\rm EOS}) = 1 - {\rm CDF}(M_{\rm max}; M_0, \sigma^2)$$

$$M_{\rm bound} = M_0 \pm \sigma$$

# Maximum Neutron Star mass

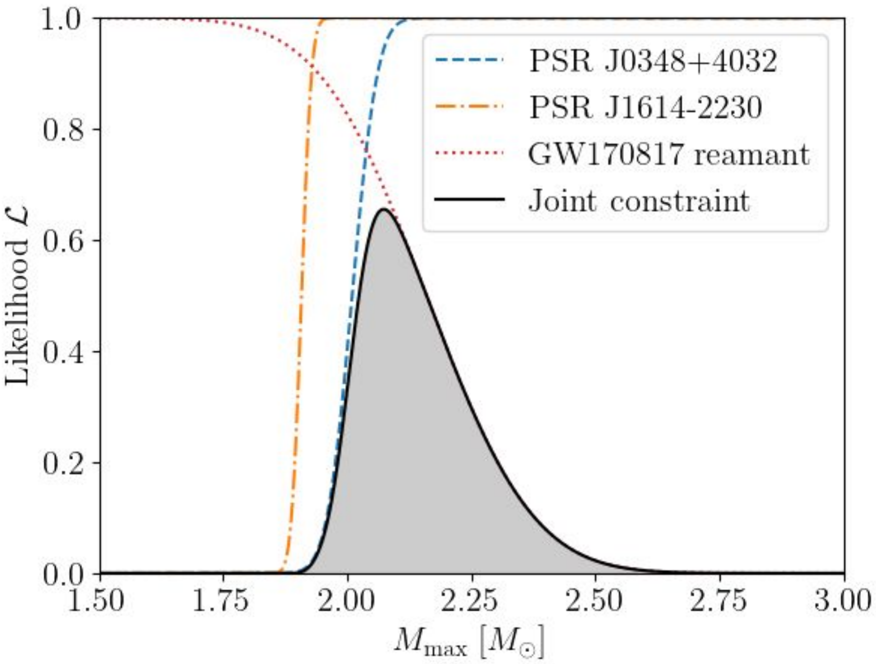


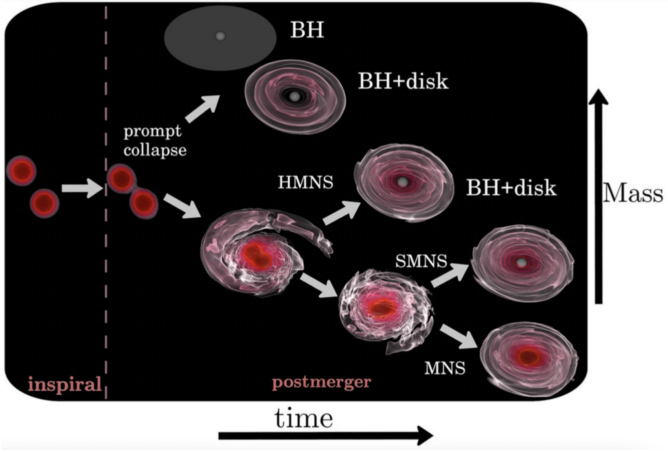


| Pulsar | Mass is $M_\odot$ |
|---|---|
| PSR J0348+4032 | $2.01 \pm 0.04$ |
| PSR J1614−2230 | $1.908 \pm 0.016$ |

# Maximum Neutron Star mass

PSR J0348+0432/PSR J1614-2230 and GW170817/AT2017gfo remnant classification

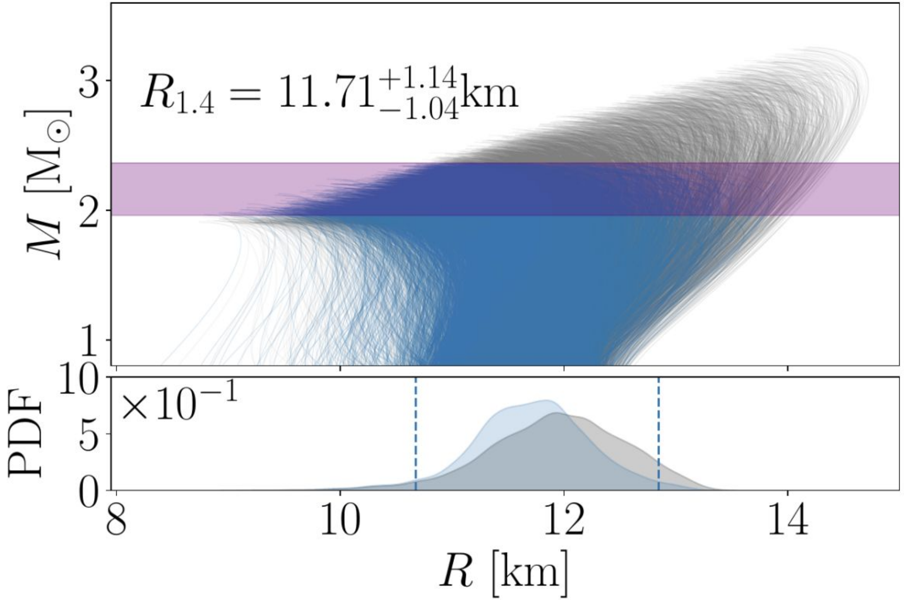


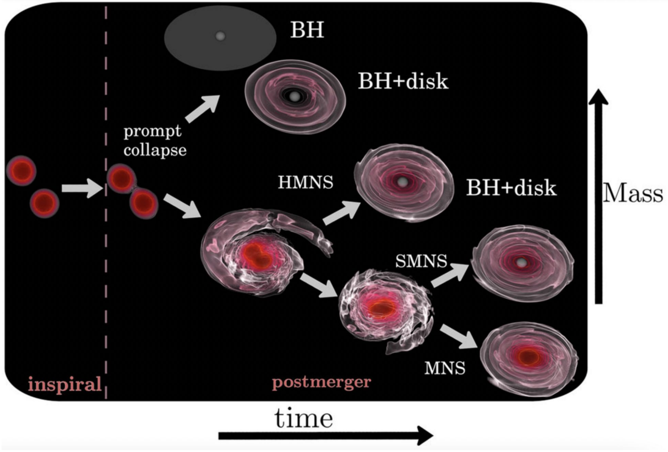


| Pulsar | Mass is $M_\odot$ |
|---|---|
| PSR J0348+4032 | $2.01 \pm 0.04$ |
| PSR J1614−2230 | $1.908 \pm 0.016$ |

# X-ray pulsar with NICER
# (The Neutron Star Interior Composition Explorer Mission)

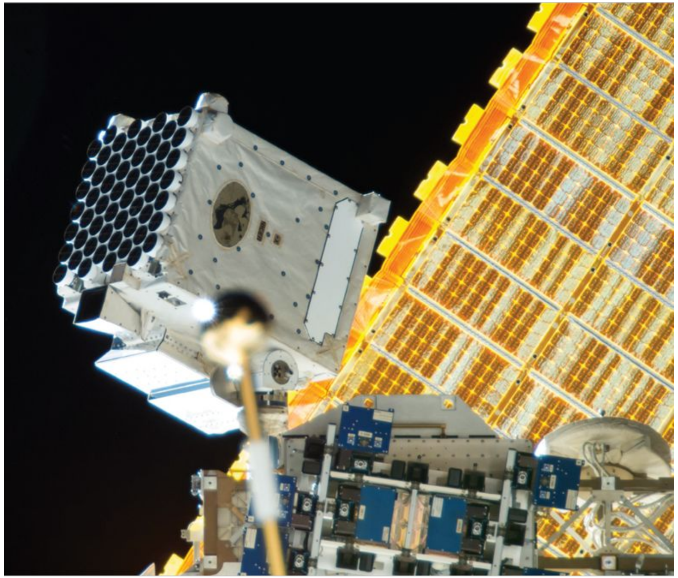

Miller et al. ApJ. Lett. 887, L24 (2019), Riley et al. ApJ. Lett. 887, L21 (2019), Miller et al. ApJ. Lett. 918, L28 (2021), Riley et al. ApJ. Lett. 918, L27 (2021)

# X-ray pulsar with NICER
# (The Neutron Star Interior Composition Explorer Mission)

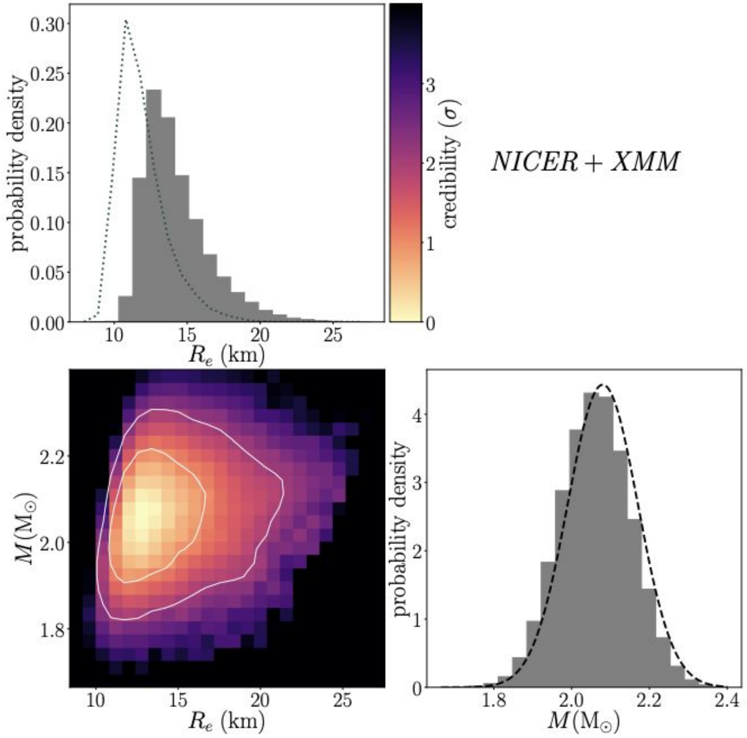


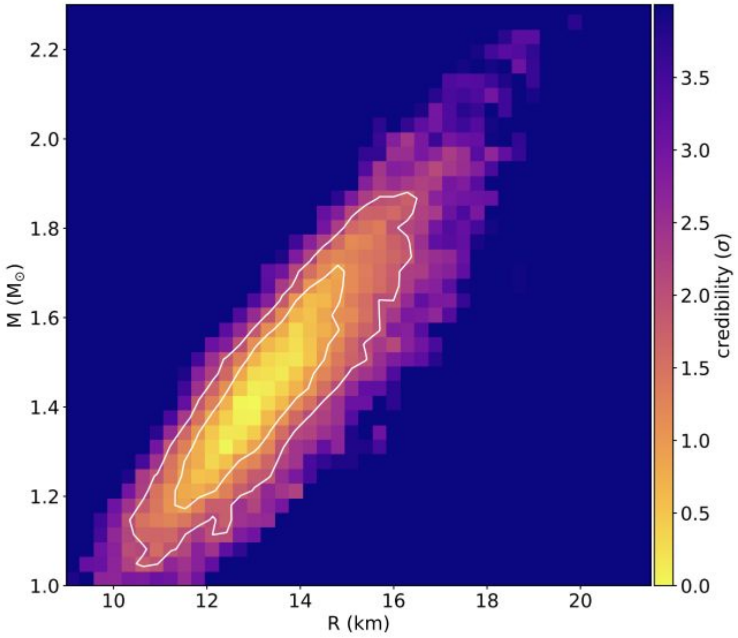


Miller et al. ApJ. Lett. 887, L24 (2019), Riley et al. ApJ. Lett. 887, L21 (2019), Miller et al. ApJ. Lett. 918, L28 (2021), Riley et al. ApJ. Lett. 918, L27 (2021)

# X-ray pulsar with NICER
# (The Neutron Star Interior Composition Explorer Mission)

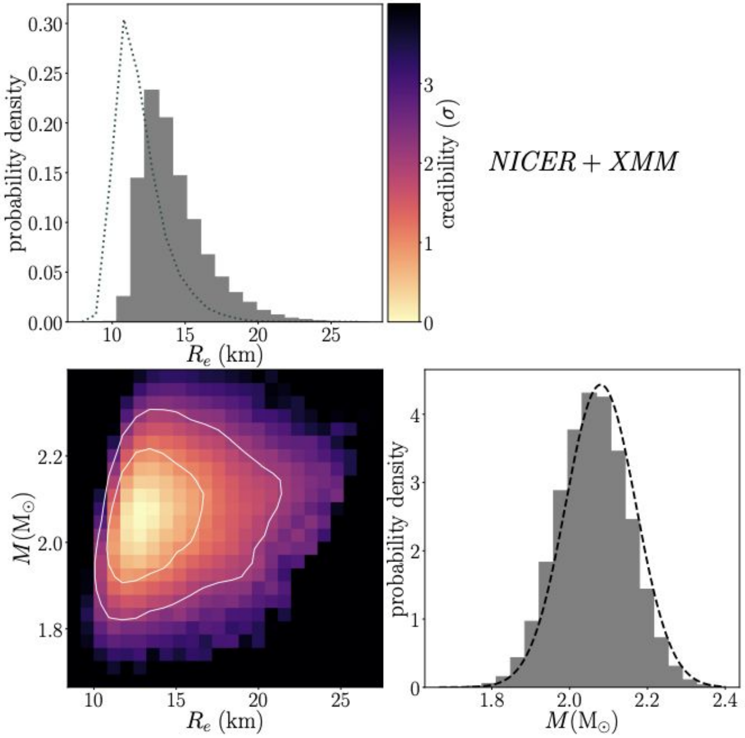


$$\mathcal{L}_{\mathrm{NICER}-j}(\mathrm{EOS})$$
$$= \int dR\, dm\, \mathcal{P}_{\mathrm{NICER}-j}(m, R) \frac{p(m, R|\mathrm{EOS})}{p(m, R|I)}$$
$$\propto \int dR\, dm\, \mathcal{P}_{\mathrm{NICER}-j}(m, R)\delta(R - R(m, \mathrm{EOS}))$$
$$\propto \int dm\, \mathcal{P}_{\mathrm{NICER}-j}(m, R = R(m, \mathrm{EOS}))\,,$$

Miller et al. ApJ. Lett. 887, L24 (2019), Riley et al. ApJ. Lett. 887, L21 (2019), Miller et al. ApJ. Lett. 918, L28 (2021), Riley et al. ApJ. Lett. 918, L27 (2021)

# X-ray pulsar with NICER
# (The Neutron Star Interior Composition Explorer Mission)

PSR J0030+0451 and PSR J0740+6620

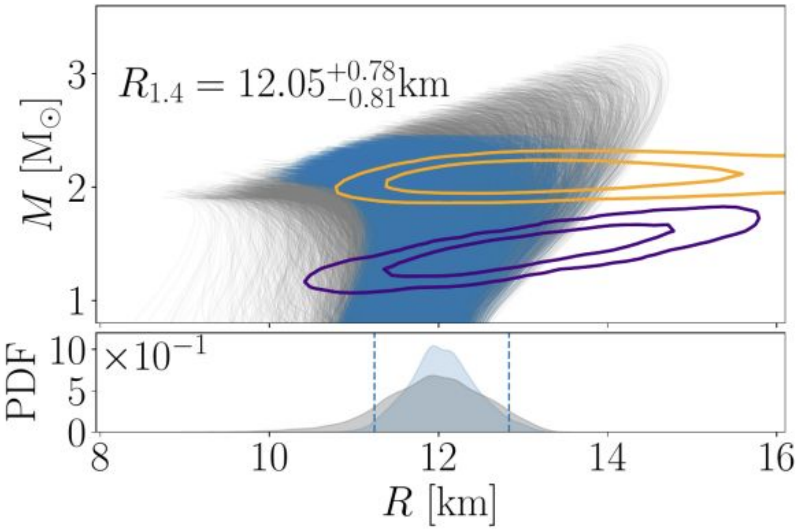


$$
\begin{aligned}
&\mathcal{L}_{\mathrm{NICER}-j}(\mathrm{EOS}) \\
&= \int dR\, dm\, \mathcal{P}_{\mathrm{NICER}-j}(m, R) \frac{p(m, R|\mathrm{EOS})}{p(m, R|I)} \\
&\propto \int dR\, dm\, \mathcal{P}_{\mathrm{NICER}-j}(m, R) \delta(R - R(m, \mathrm{EOS})) \\
&\propto \int dm\, \mathcal{P}_{\mathrm{NICER}-j}(m, R = R(m, \mathrm{EOS}))\,,
\end{aligned}
$$

Miller et al. ApJ. Lett. 887, L24 (2019), Riley et al. ApJ. Lett. 887, L21 (2019), Miller et al. ApJ. Lett. 918, L28 (2021), Riley et al. ApJ. Lett. 918, L27 (2021)

# Gravitational waves

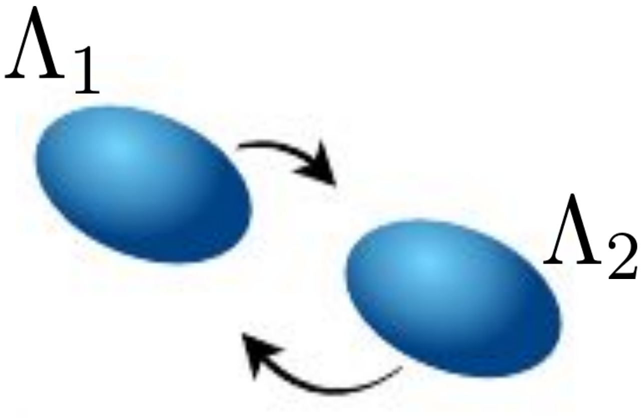


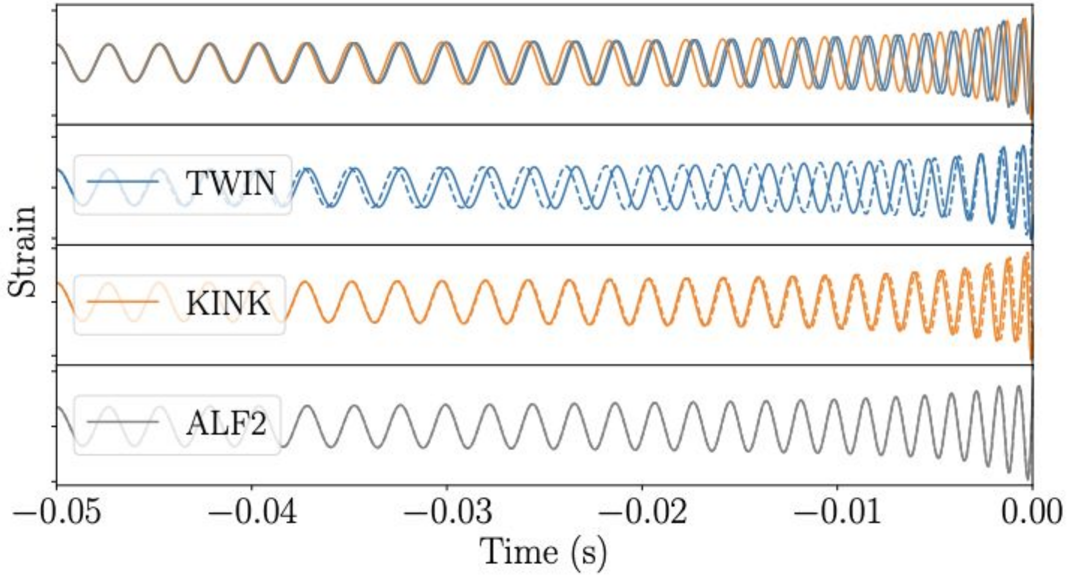

# Gravitational waves

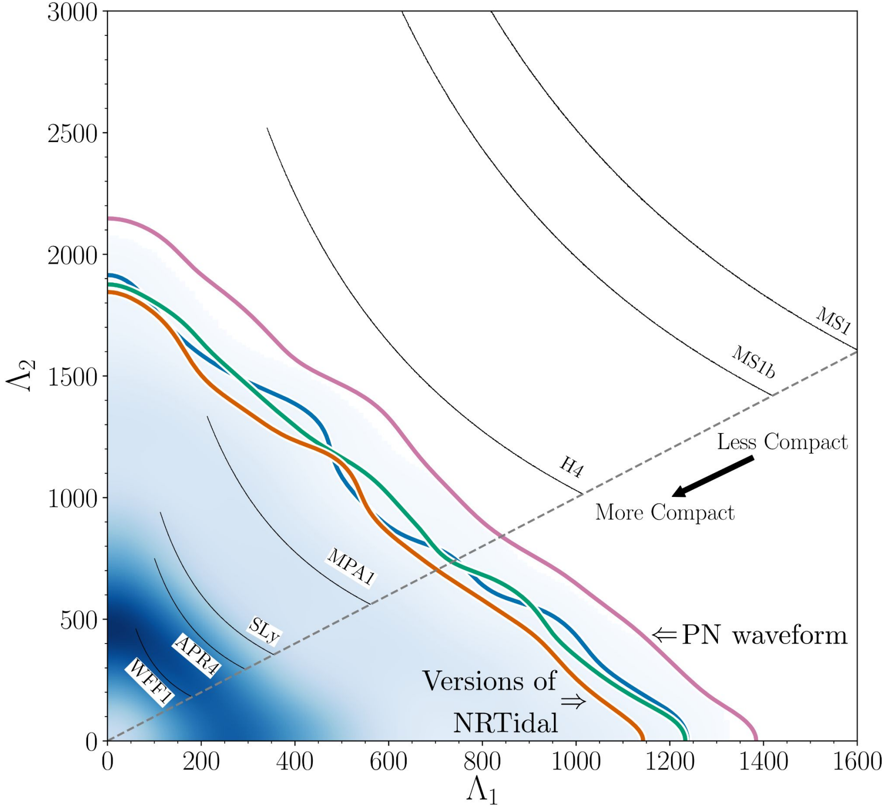


$$\mathcal{L}_{\rm GW} \propto \exp\left(-2\int df \frac{|\tilde{d}(f) - \tilde{h}(f; {\rm EOS}, \vec{\theta})|^2}{S_n(f)}\right)$$

- 15 source parameters + 1 EOS
- 20 * number of detector => calibration parameters
- Markov chain Monte Carlo / Nested sampling used for high-dimensional exploration

# Gravitational waves

**GW170817:**
reanalysis with
IMRPhenomPv2_NRTidalv2

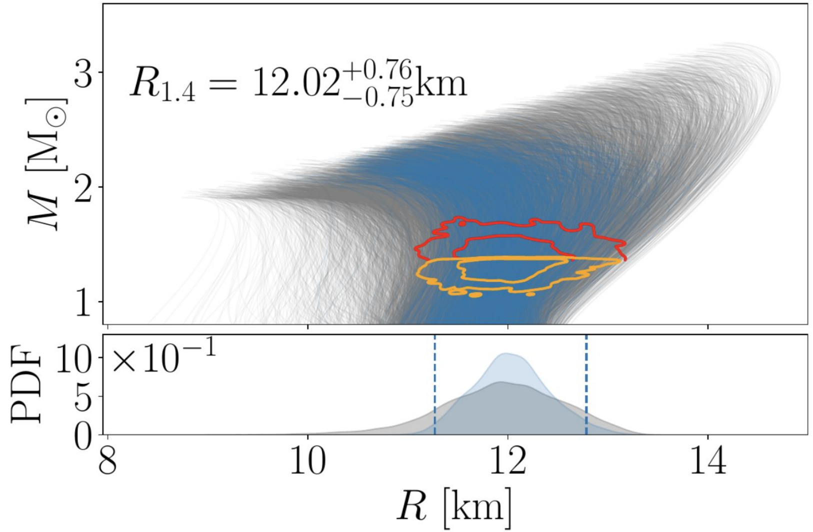


**GW190425:**
reanalysis with
IMRPhenomPv2_NRTidalv2

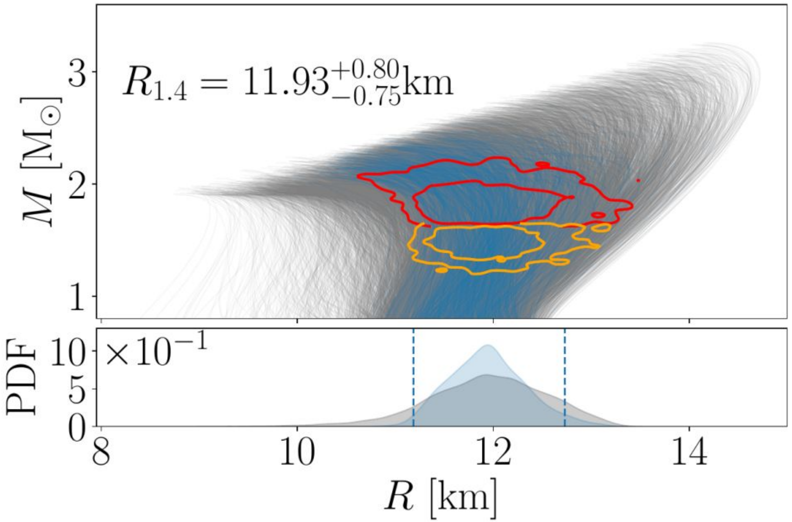

# Kilonovae

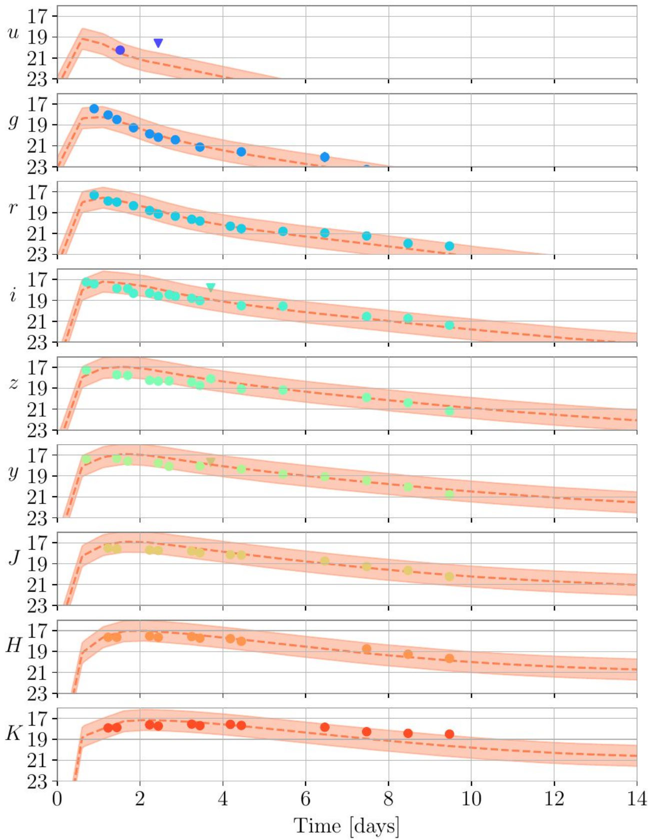


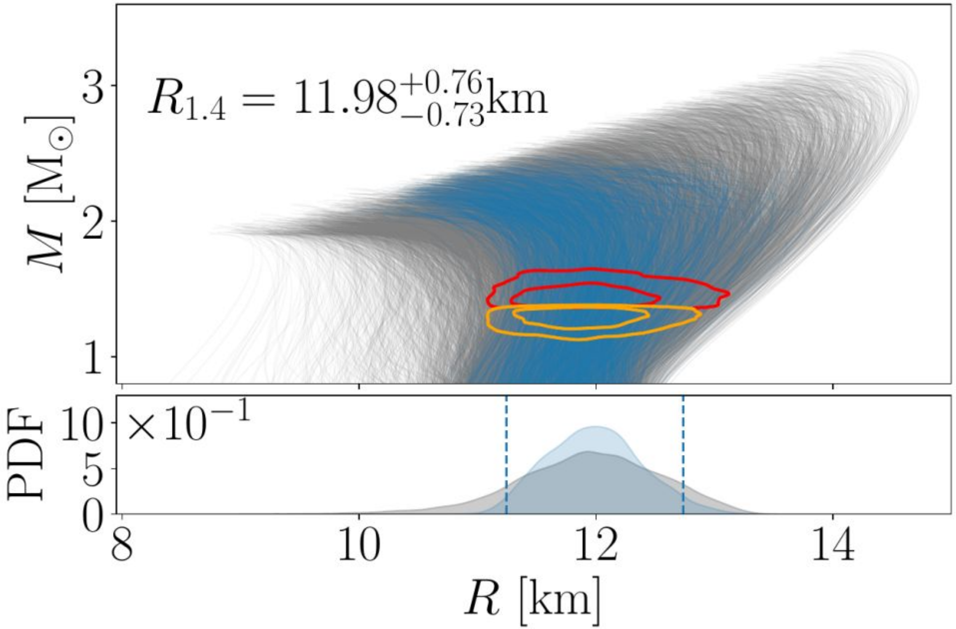


$$\mathcal{L}_{\mathrm{EM}} \propto \exp\left(-\frac{1}{2}\sum_{ij}\left(\frac{m_i^j - m_i^{j,\mathrm{est}}(\mathrm{EOS}, \vec{\theta})}{\sigma_i^j}\right)^2\right)$$

# Heavy-ion collisions

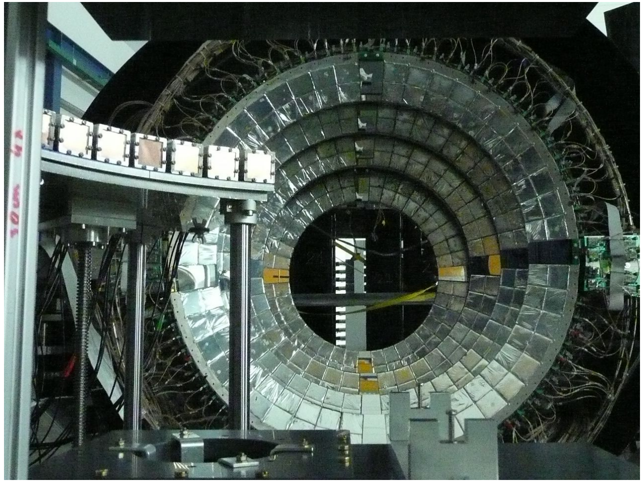

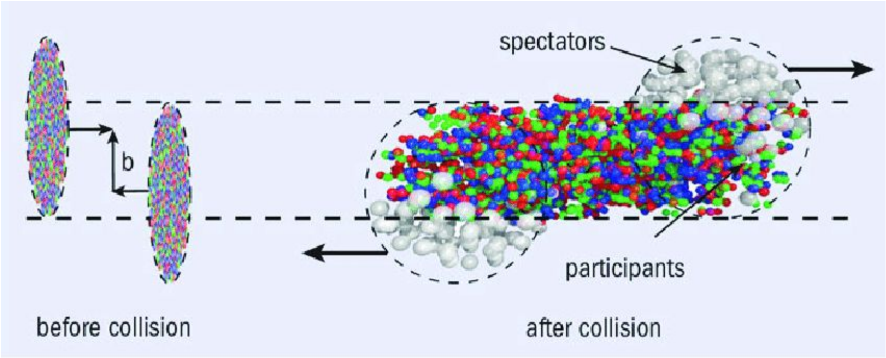


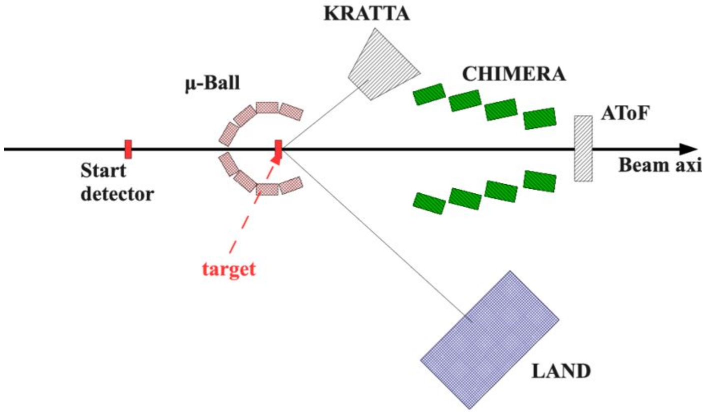

**Symmetric matter**

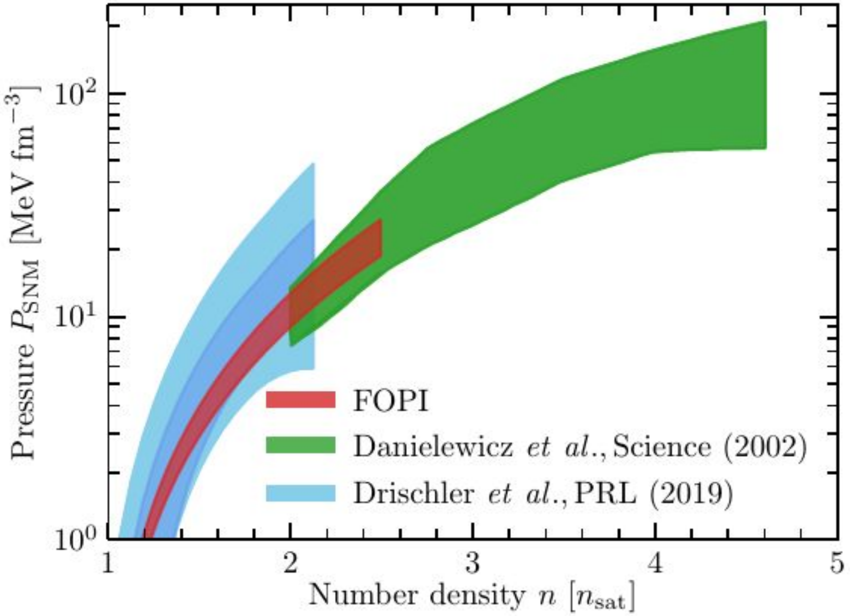


**Asymmetric matter**

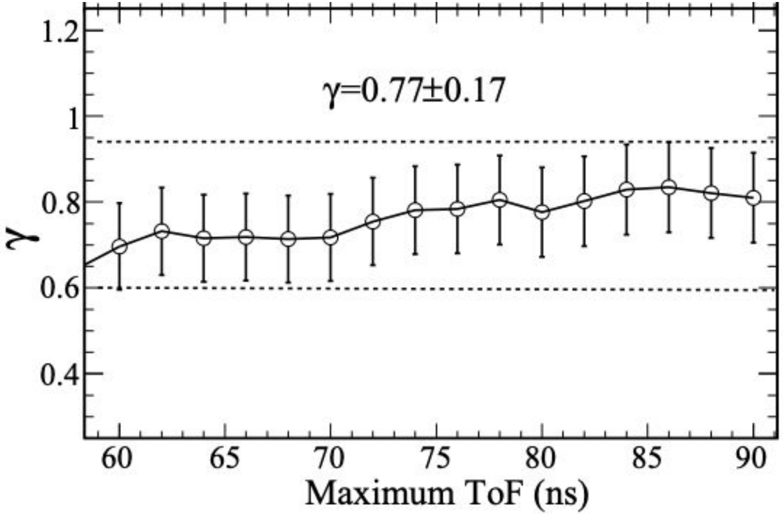

**EOS functional**

$$\frac{E}{A}(n,\delta) \approx \frac{E}{A}(n,0) + S(n)\delta^2$$

$$\frac{E}{A}(n,0) = \frac{3}{5}\left(\frac{n}{n_{\rm sat}}\right)^{\frac{2}{3}} E_{\rm F} + \frac{\alpha n}{2n_{\rm sat}} + \frac{\beta}{\gamma+1}\left(\frac{n}{n_{\rm sat}}\right)^{\gamma}$$

$$S(n) = E_{\rm kin,0}\left(\frac{n}{n_{\rm sat}}\right)^{\frac{2}{3}} + E_{\rm pot,0}\left(\frac{n}{n_{\rm sat}}\right)^{\gamma_{\rm asy}}$$

$$P(n,\delta) = n^2 \frac{\partial E/A(n,\delta)}{\partial n}$$

**Sensitivity**

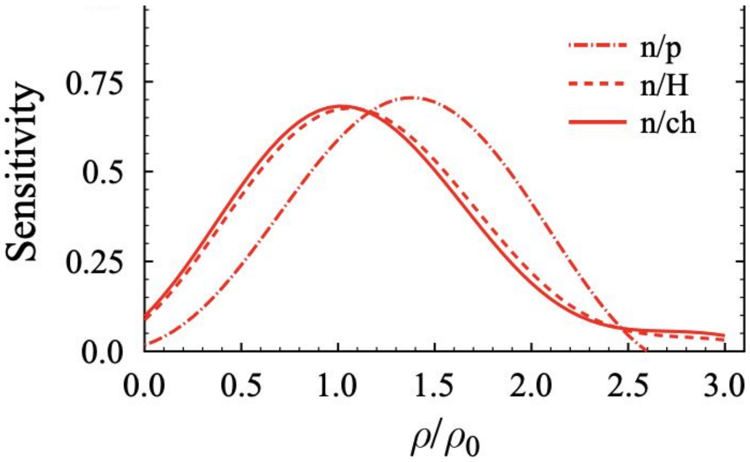

**HIC experiments:**

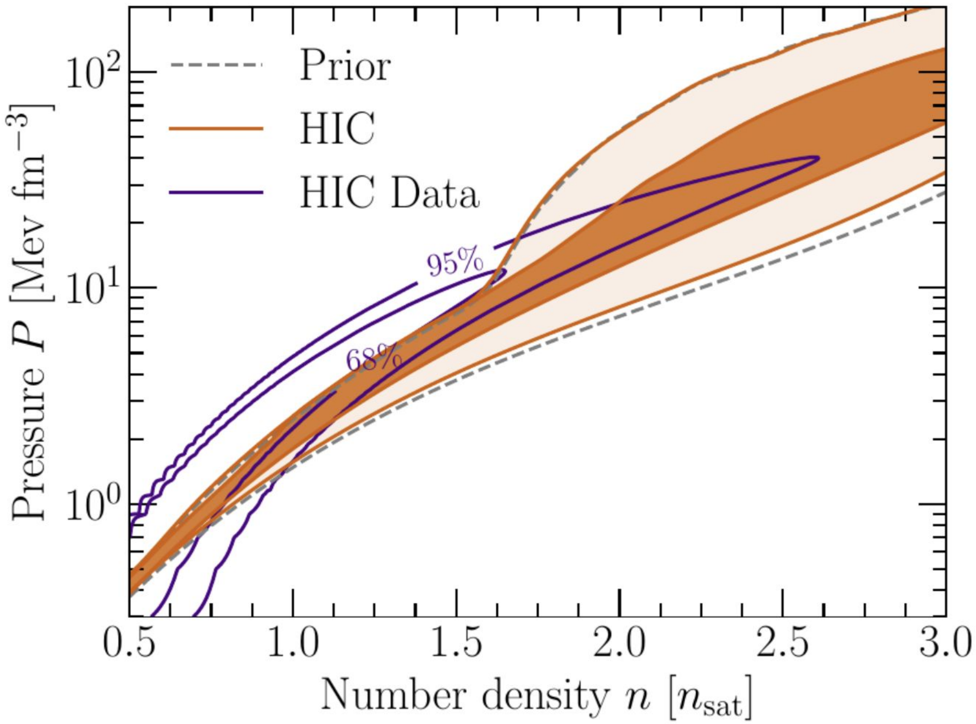


$$\mathcal{L}_{\rm HIC}({\rm EOS})$$
$$= \int dn\, dP\ p({\rm HIC}|n, P)p(n, P|{\rm EOS})$$
$$= \int dn\, P(n, P = P(n; {\rm EOS})|{\rm HIC})$$

# Combing information

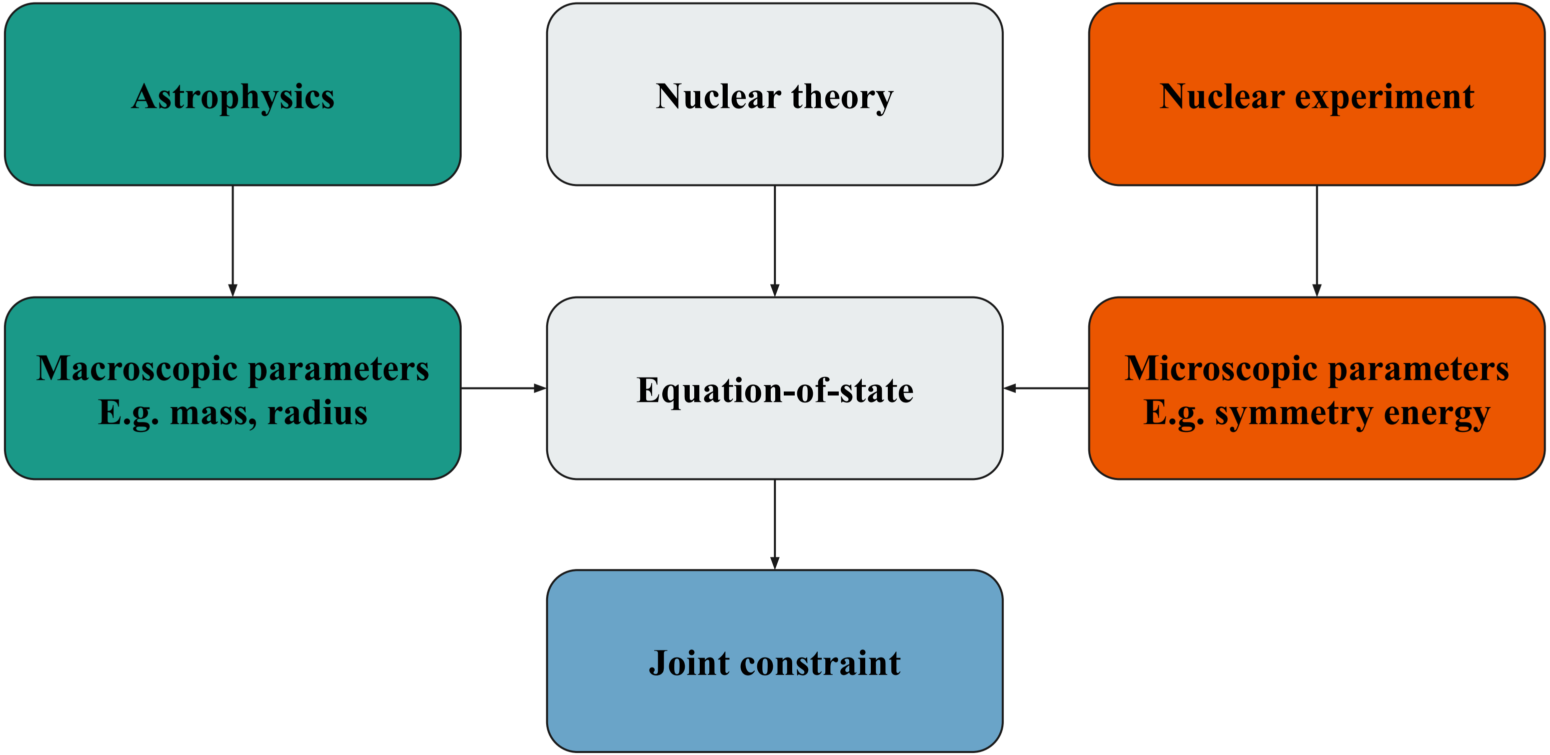

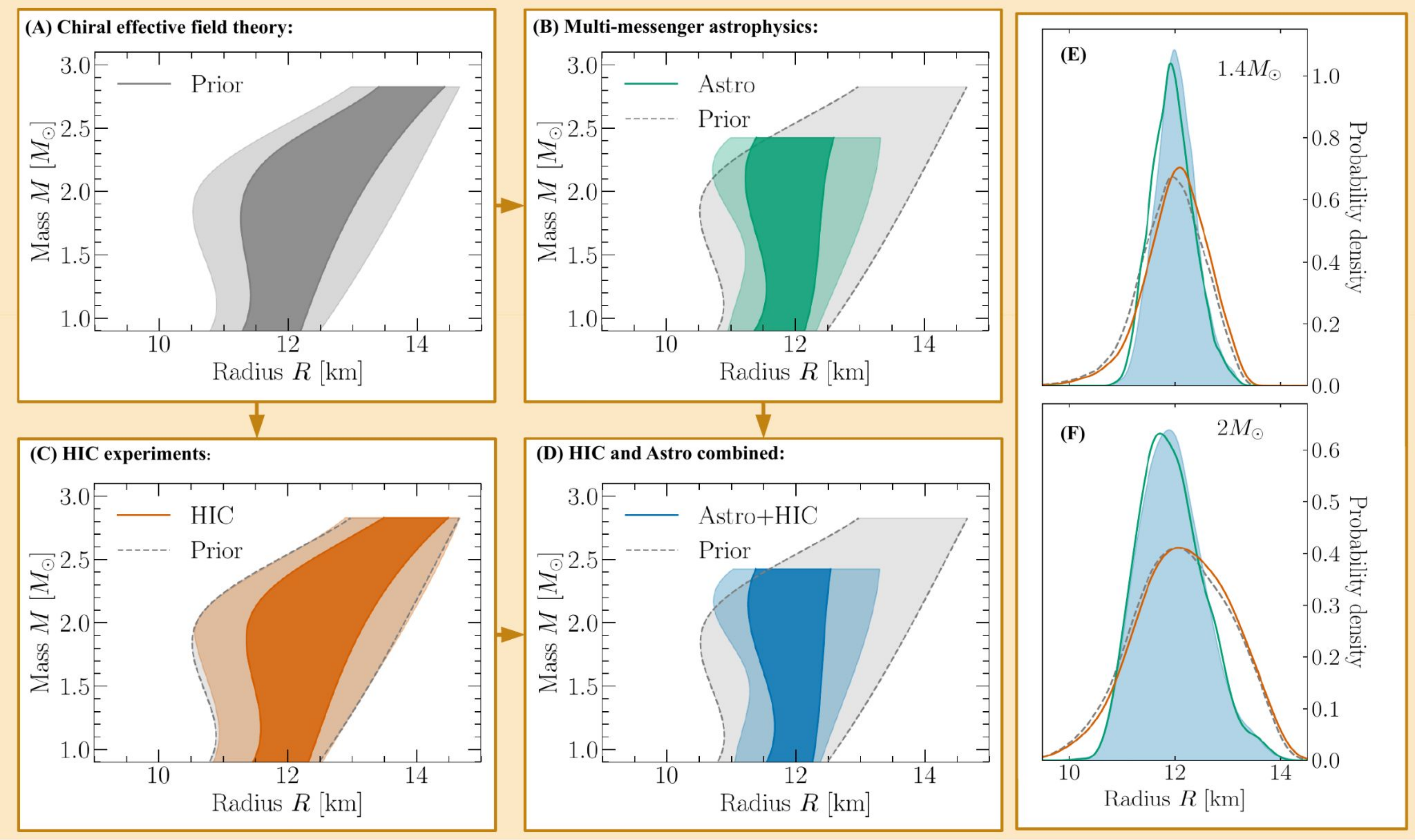

(A) Chiral effective field theory:
Prior
Mass M [M⊙]
Radius R [km]
(B) Multi-messenger astrophysics:
Astro
Prior
(C) HIC experiments:
HIC
Prior
(D) HIC and Astro combined:
Astro+HIC
Prior
(E)
1.4M⊙
(F)
2M⊙
Probability density

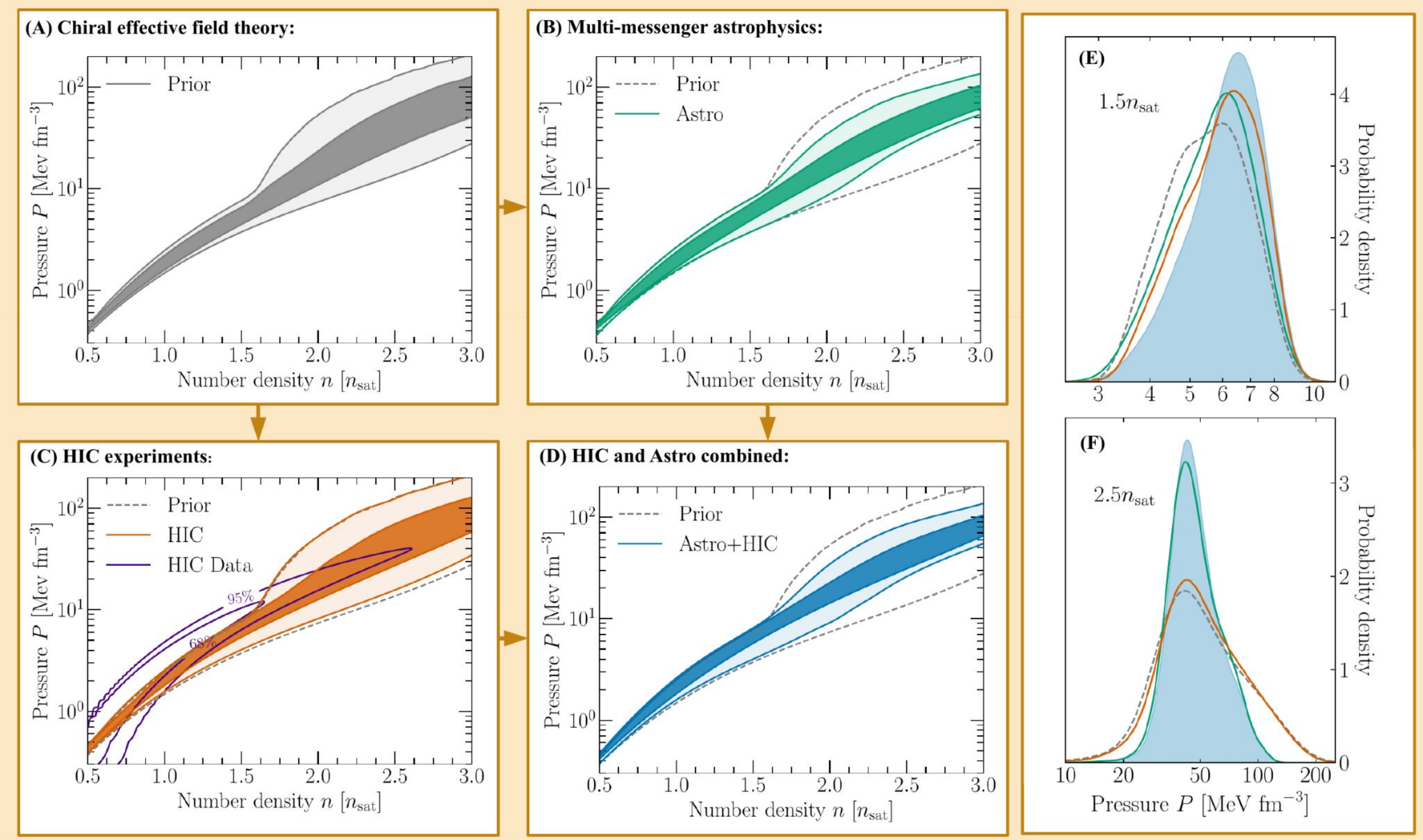
(A) Chiral effective field theory:
Prior
Pressure $P$ [Mev fm$^{-3}$]
Number density $n$ [$n_{sat}$]
(B) Multi-messenger astrophysics:
Prior
Astro
Pressure $P$ [Mev fm$^{-3}$]
Number density $n$ [$n_{sat}$]
(C) HIC experiments:
Prior
HIC
HIC Data
95%
68%
Pressure $P$ [Mev fm$^{-3}$]
Number density $n$ [$n_{sat}$]
(D) HIC and Astro combined:
Prior
Astro+HIC
Pressure $P$ [Mev fm$^{-3}$]
Number density $n$ [$n_{sat}$]
(E)
$1.5n_{sat}$
Probability density
(F)
$2.5n_{sat}$
Probability density
Pressure $P$ [MeV fm$^{-3}$]

# Result

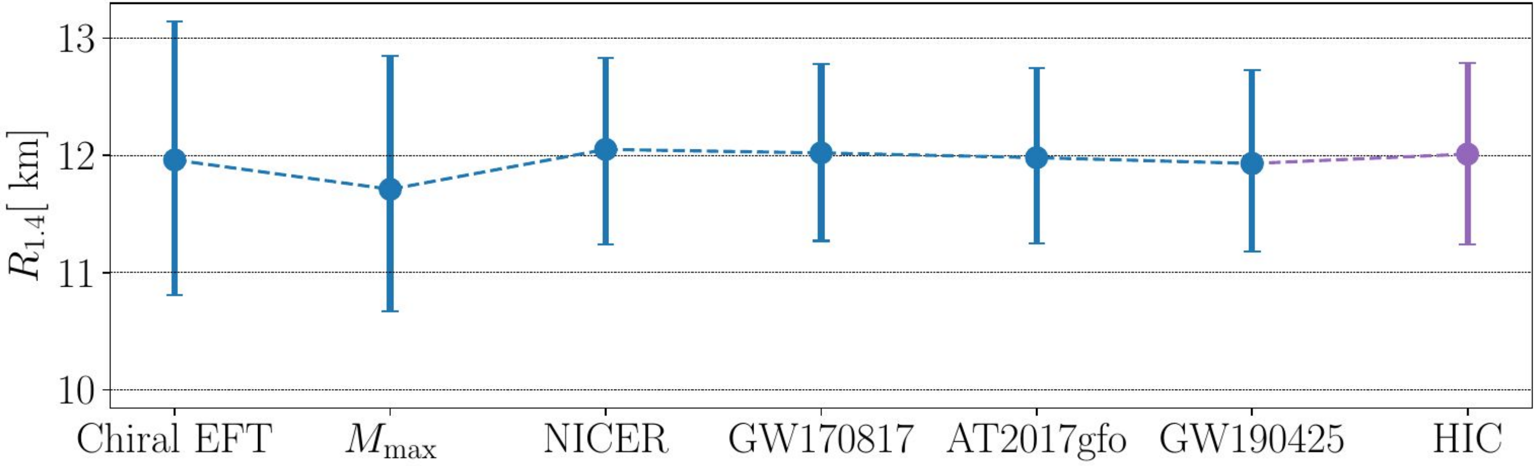


| | Prior (CEFT) | Astro+CEFT | HIC+CEFT | Combined |
|---|---|---|---|---|
| $P_{1.5n_{\rm sat}}$ [MeVfm$^{-3}$] | $5.59^{+2.04}_{-1.97}$ | $5.84^{+1.95}_{-2.26}$ | $6.06^{+1.85}_{-2.04}$ | $6.25^{+1.90}_{-2.26}$ |
| $R_{1.4}$ [km] | $11.96^{+1.18}_{-1.15}$ | $11.93^{+0.80}_{-0.75}$ | $12.06^{+1.13}_{-1.18}$ | $12.01^{+0.78}_{-0.77}$ |

# What is the next step?

# What is the next step?

Nuclear experiments

Astrophysical modelling

Nuclear theory

Joint analysis

# What is the next step?

Joint analysis

# NMMA

**Nuclear Physics and Multi-messenger Astrophysics**

github.com/nuclear-multimessenger-astronomy/nmma

# NMMA

- Simultaneously analyzing GW, kilonova and GRB afterglow
- Fully capture the correlation between parameters
- HPC facilities needed

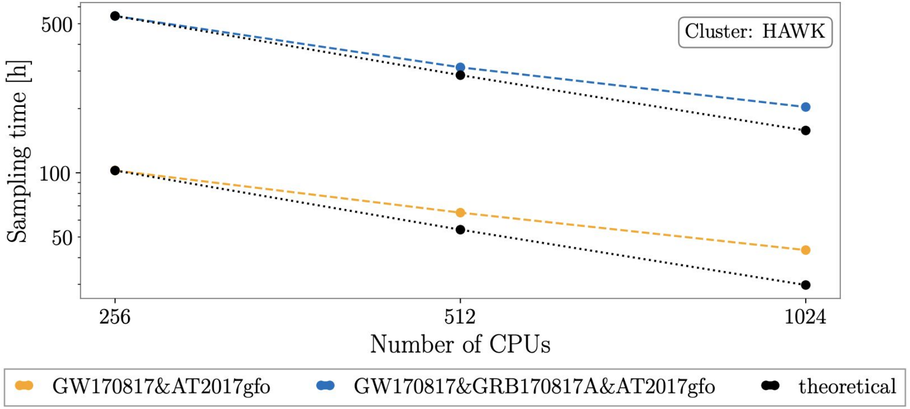


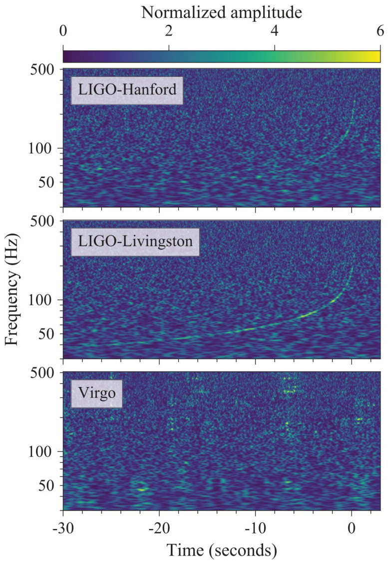


+

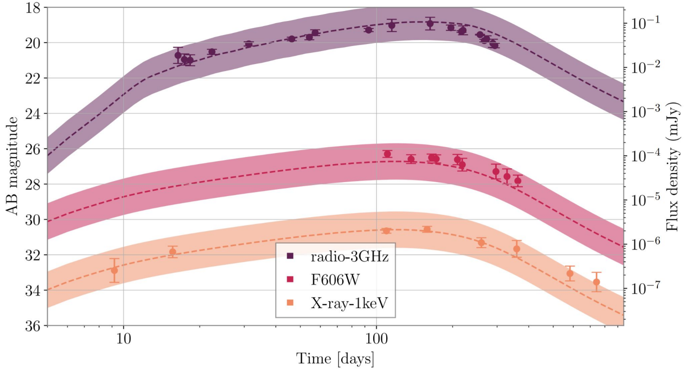


+

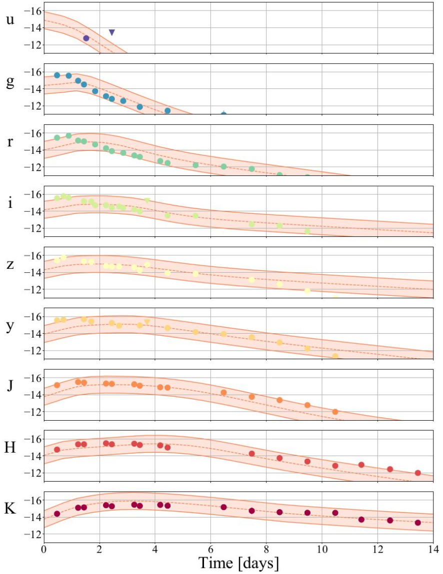

# NMMA

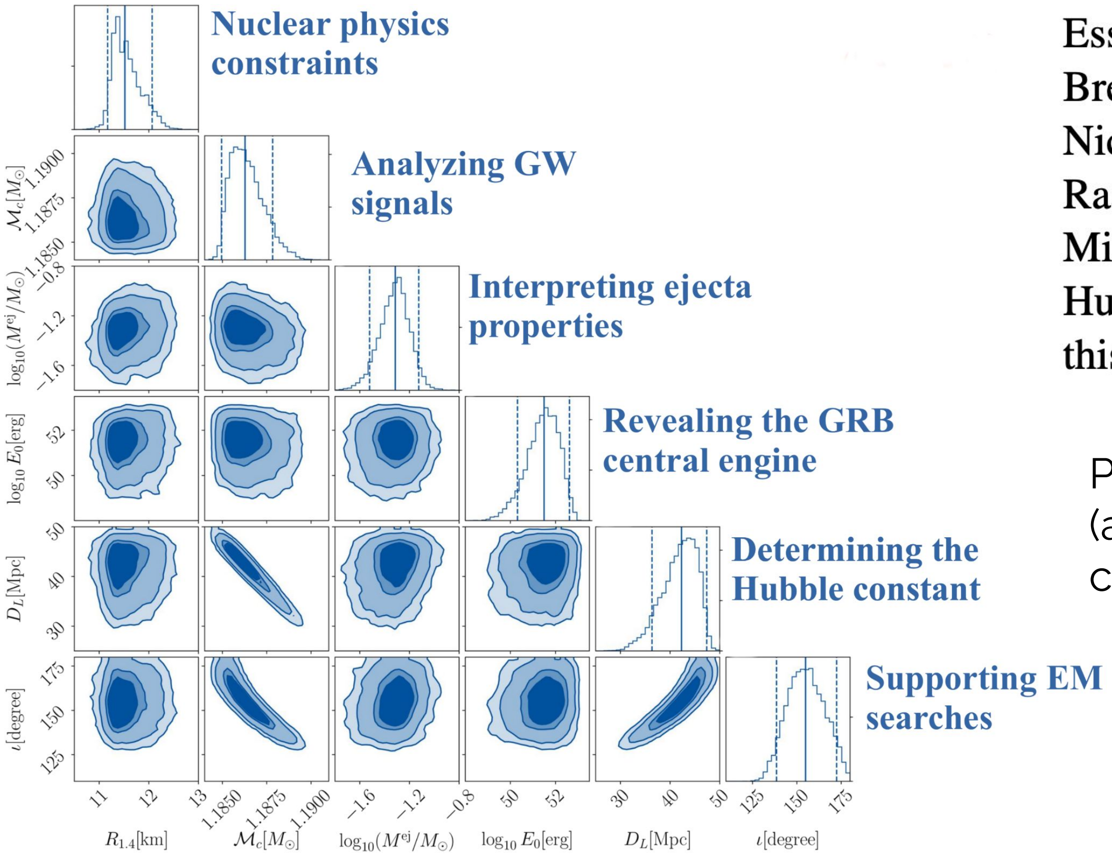


| Reference | $R_{1.4M_\odot}$ [km] |
|---|---|
| Dietrich et al. [15] | $11.75^{+0.86}_{-0.81}$ (90%) |
| Essick et al. [51] | $12.54^{+0.71}_{-0.63}$ (90%) |
| Breschi et al. [23] | $11.99^{+0.82}_{-0.85}$ (90%) |
| Nicholl et al. [24] | $11.06^{+1.01}_{-0.98}$ (90%) |
| Raaijmakers et al. [25] | $12.18^{+0.56}_{-0.79}$ (95%) |
| Miller et al. [52] | $12.45^{+0.65}_{-0.65}$ (68%) |
| Huth et al. [16] | $12.01^{-0.78}_{-0.77}$ (90%) |
| this work [NMMA][53] | $11.98^{+0.35}_{-0.40}$ (90%) |

Pang et al. arxiv: 2205.08513 (accepted by Nature communication)

# Application: GRB211211A (Kunert et al. arxiv:2301.02049)

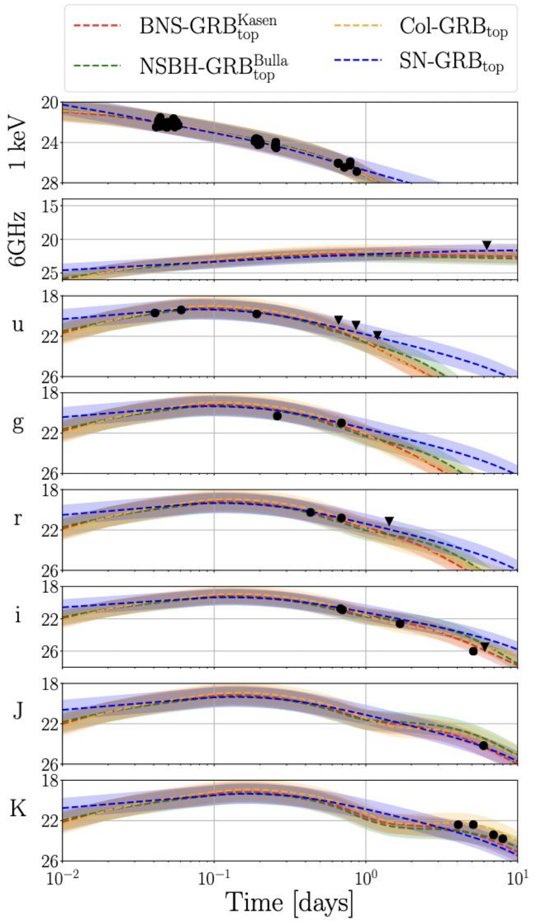


| Name | Astrophysical Processes | Bayes factor $\ln[\mathcal{B}^{1}_{\rm ref}]$ | Likelihood $\ln[\mathcal{L}^{1}_{\rm ref}(\hat{\theta})]$ |
|---|---|---|---|
| BNS-GRB$^{\rm Kasen}_{\rm top}$ | Kilonova + GRB | ref. | ref. |
| BNS-GRB$^{\rm Kasen}_{\rm Gauss}$ | Kilonova + GRB | -1.01 ± 0.10 | -0.33 |
| BNS-GRB$^{\rm Bulla}_{\rm top}$ | Kilonova + GRB | -0.49 ± 0.10 | -1.15 |
| BNS-GRB$^{\rm Bulla}_{\rm Gauss}$ | Kilonova + GRB | -1.59 ± 0.10 | -2.13 |
| NSBH-GRB$_{\rm top}$ | Kilonova + GRB | -3.76 ± 0.10 | -3.82 |
| NSBH-GRB$_{\rm Gauss}$ | Kilonova + GRB | -2.08 ± 0.10 | -4.16 |
| SNCol-GRB$_{\rm top}$ | $r$CCSNe + GRB | -10.42 ± 0.11 | -3.04 |
| SNCol-GRB$_{\rm Gauss}$ | $r$CCSNe + GRB | -10.74 ± 0.11 | -3.58 |
| SN98bw-GRB$_{\rm top}$ | CCSNe + GRB | -6.93 ± 0.10 | -8.14 |
| SN98bw-GRB$_{\rm Gauss}$ | CCSNe + GRB | -8.05 ± 0.10 | -8.13 |
| GRB$_{\rm top}$ | GRB | -6.04 ± 0.10 | -7.10 |
| GRB$_{\rm Gauss}$ | GRB | -6.96 ± 0.10 | -7.33 |

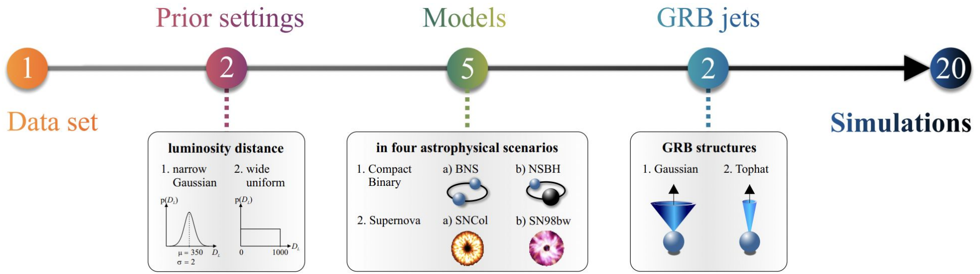

NMMA

# Application: GRB211211A (Kunert et al. arxiv:2301.02049)

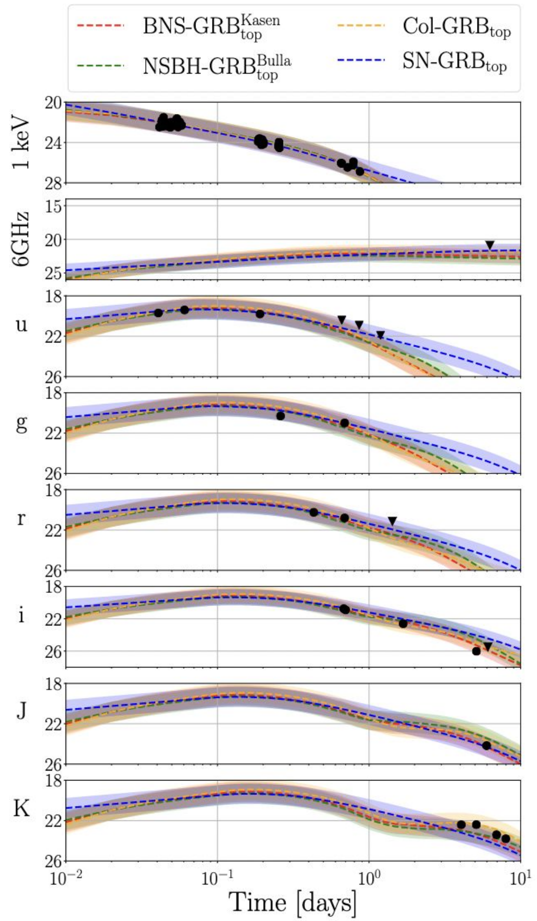


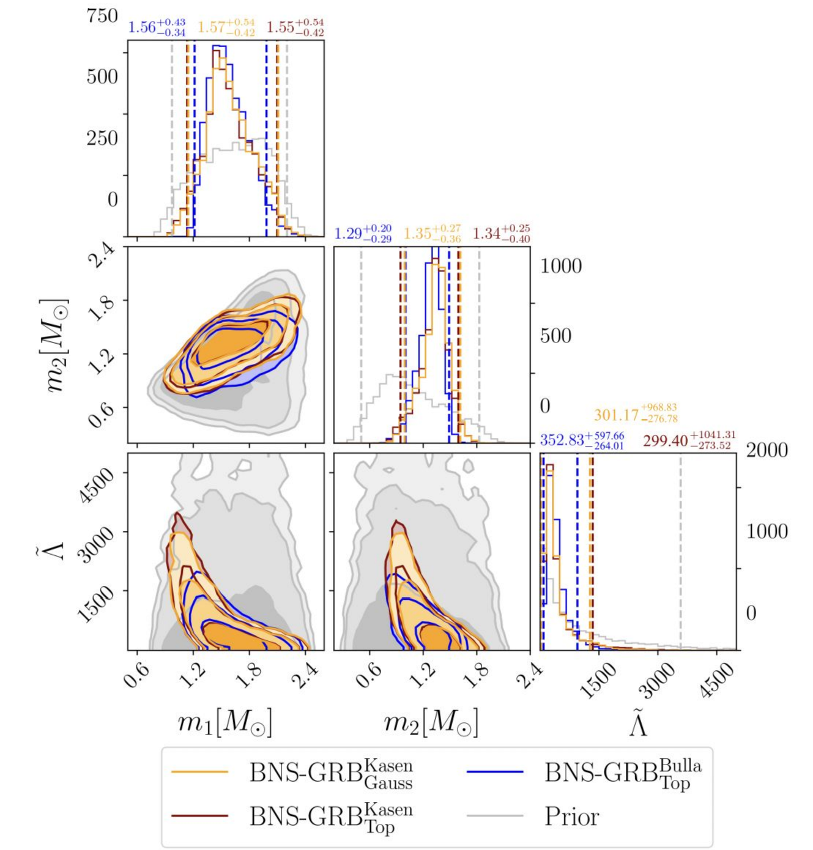

# NMMA Application: GW190814 (Tews et al. ApJL 908(2021) 1, L1)

- If GW170817 produced a BH:
  - GW190814 is a BBH with > 99.9%

- relaxing this assumption:
  - GW190814 is a BBH with ~ 83%

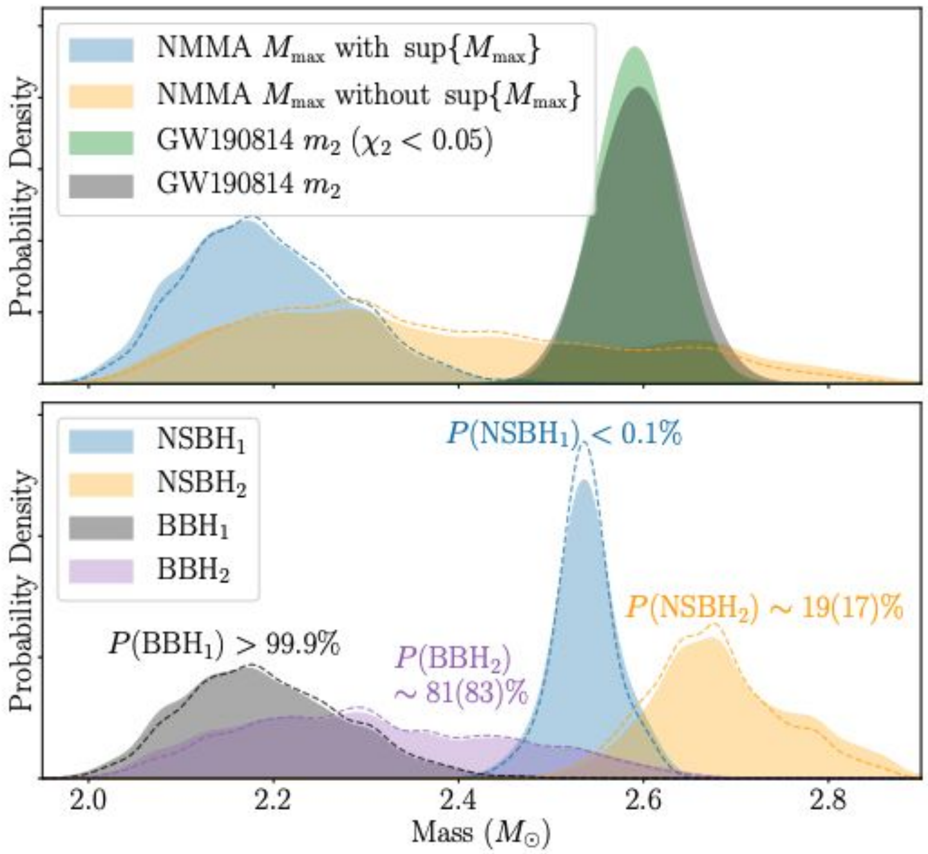

# Application: GW190814 (Tews et al. ApJL 908(2021) 1, L1)

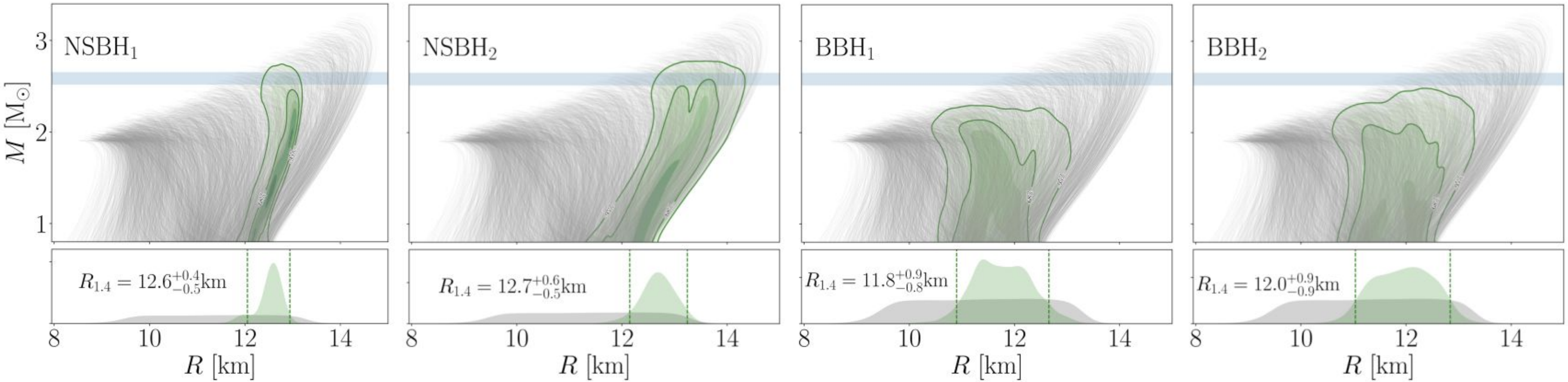

NMMA

# Multimessenger constraint on quarkyonic model (Pang et al. arxiv:2308.15067)

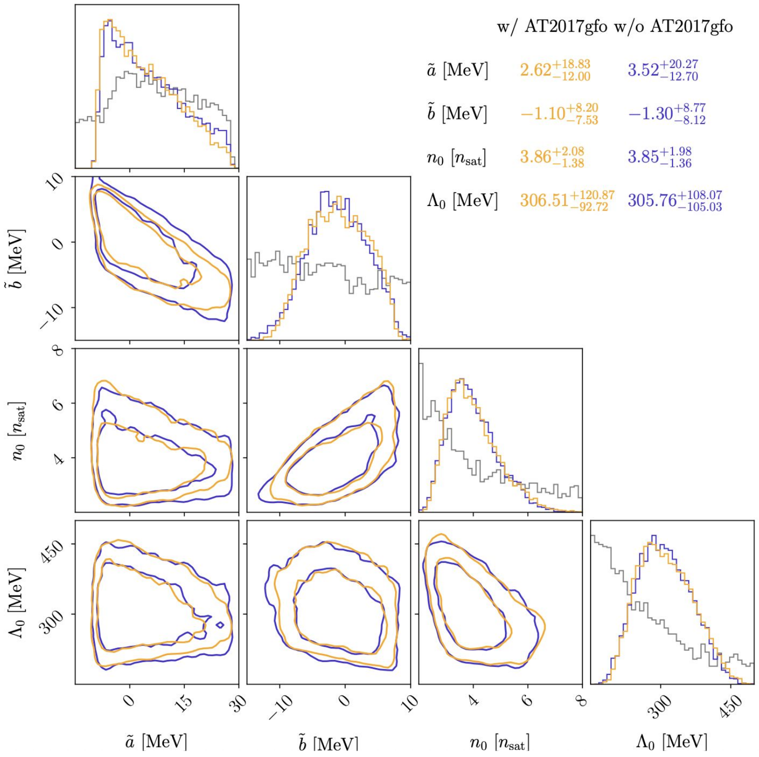


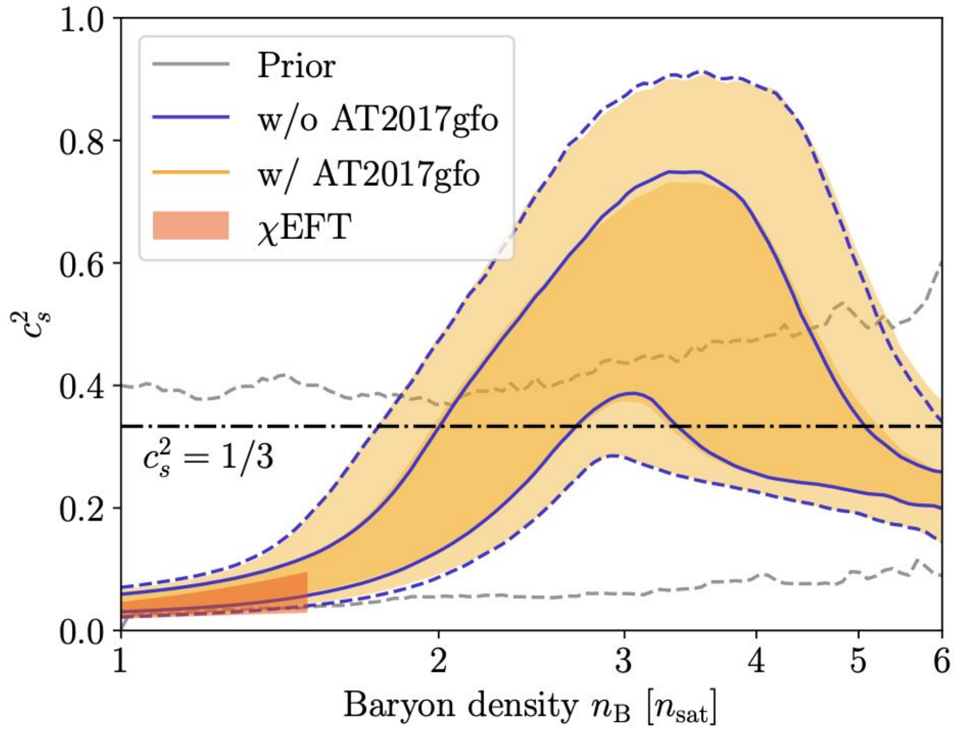

# What is the next step?

# What is the next step?

Nuclear theory

Nuclear experiments

Astrophysical modelling

# WE NEED YOU!!

How to reliably improve the interdisciplinary / multi-messenger study on supranuclear matter?

# X-ray / radio pulsar

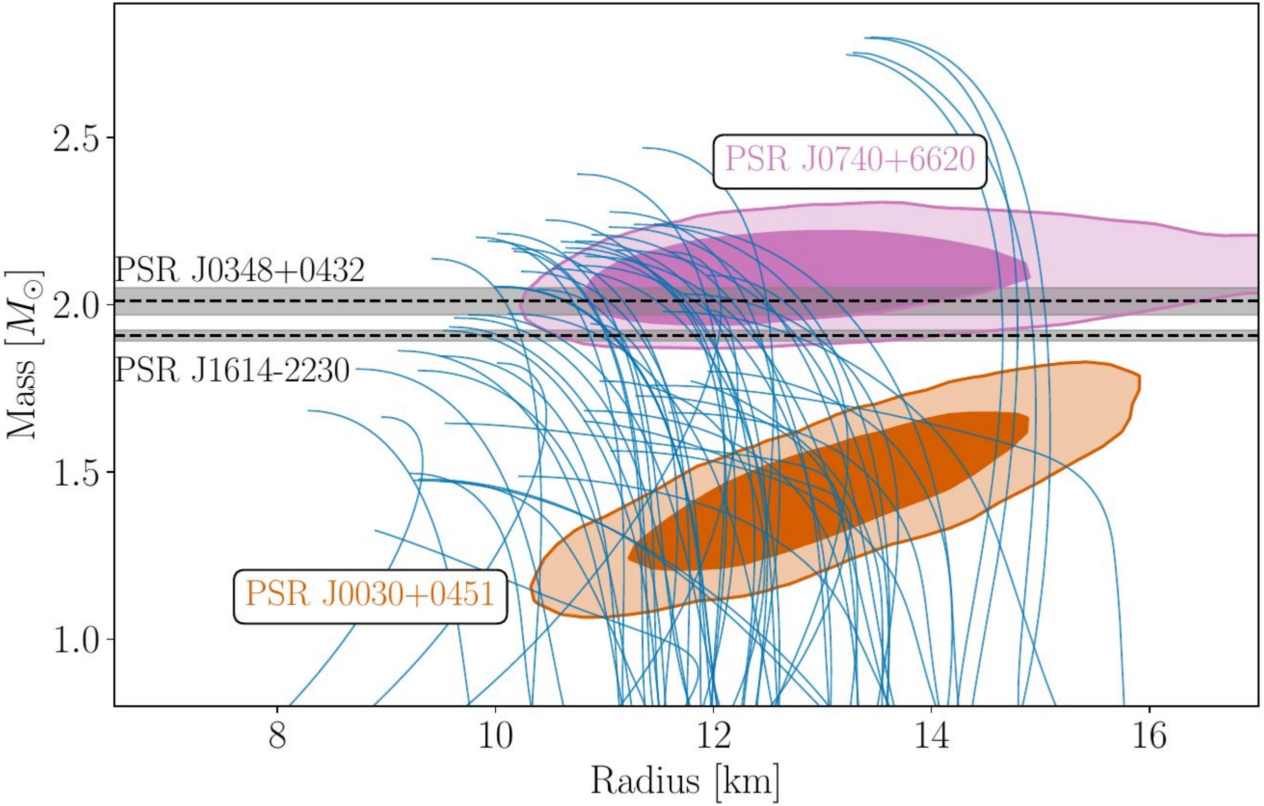

## Gravitational-waves

$$Q_{ij} = -\Lambda m^5 \mathcal{E}_{ij}$$

$$\Lambda = \frac{2}{3} k_2 \left( \frac{R}{m} \right)^5,$$

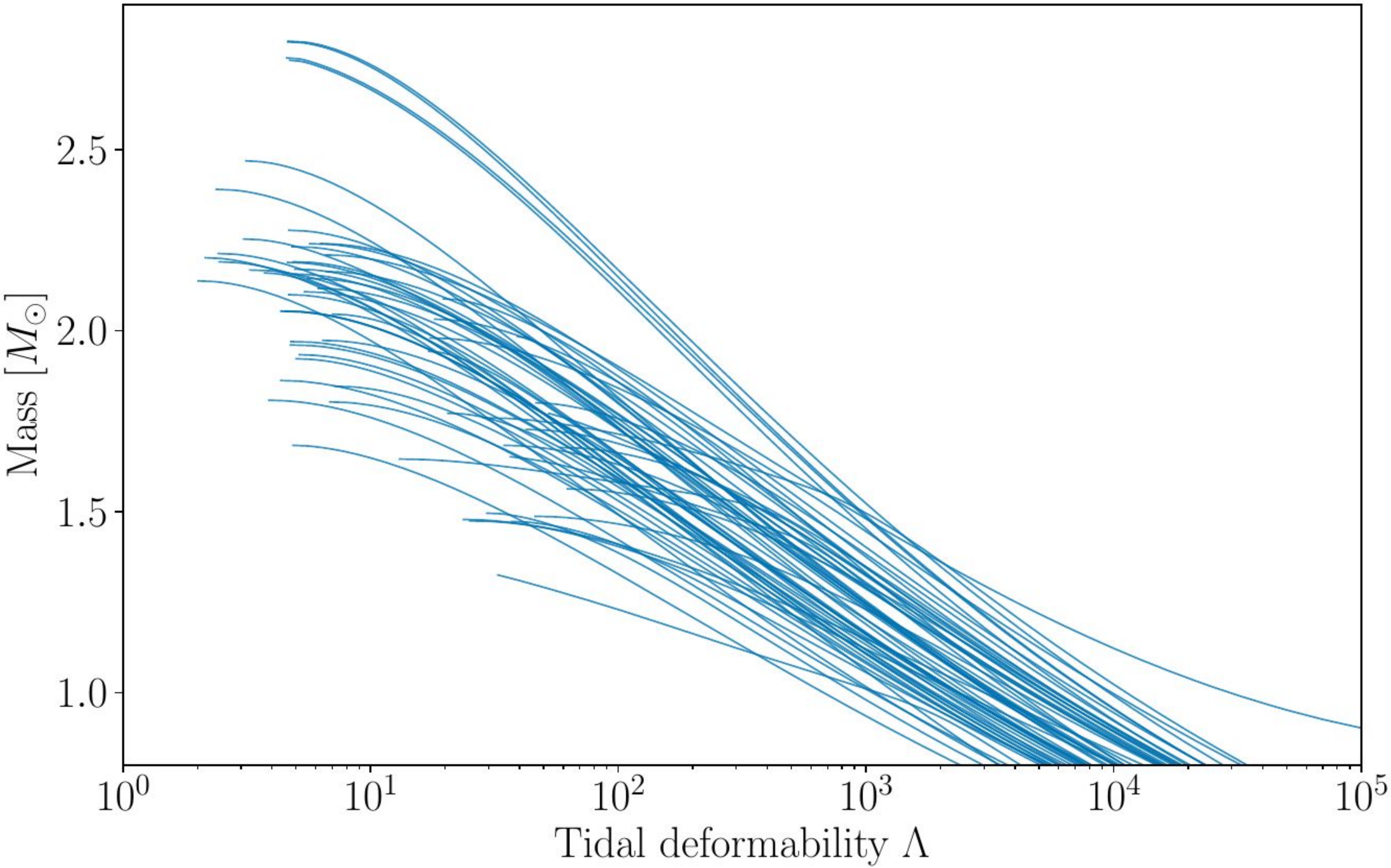

Mass $[M_\odot]$
2.5
2.0
1.5
1.0
$10^0$
$10^1$
$10^2$
$10^3$
$10^4$
$10^5$
Tidal deformability $\Lambda$

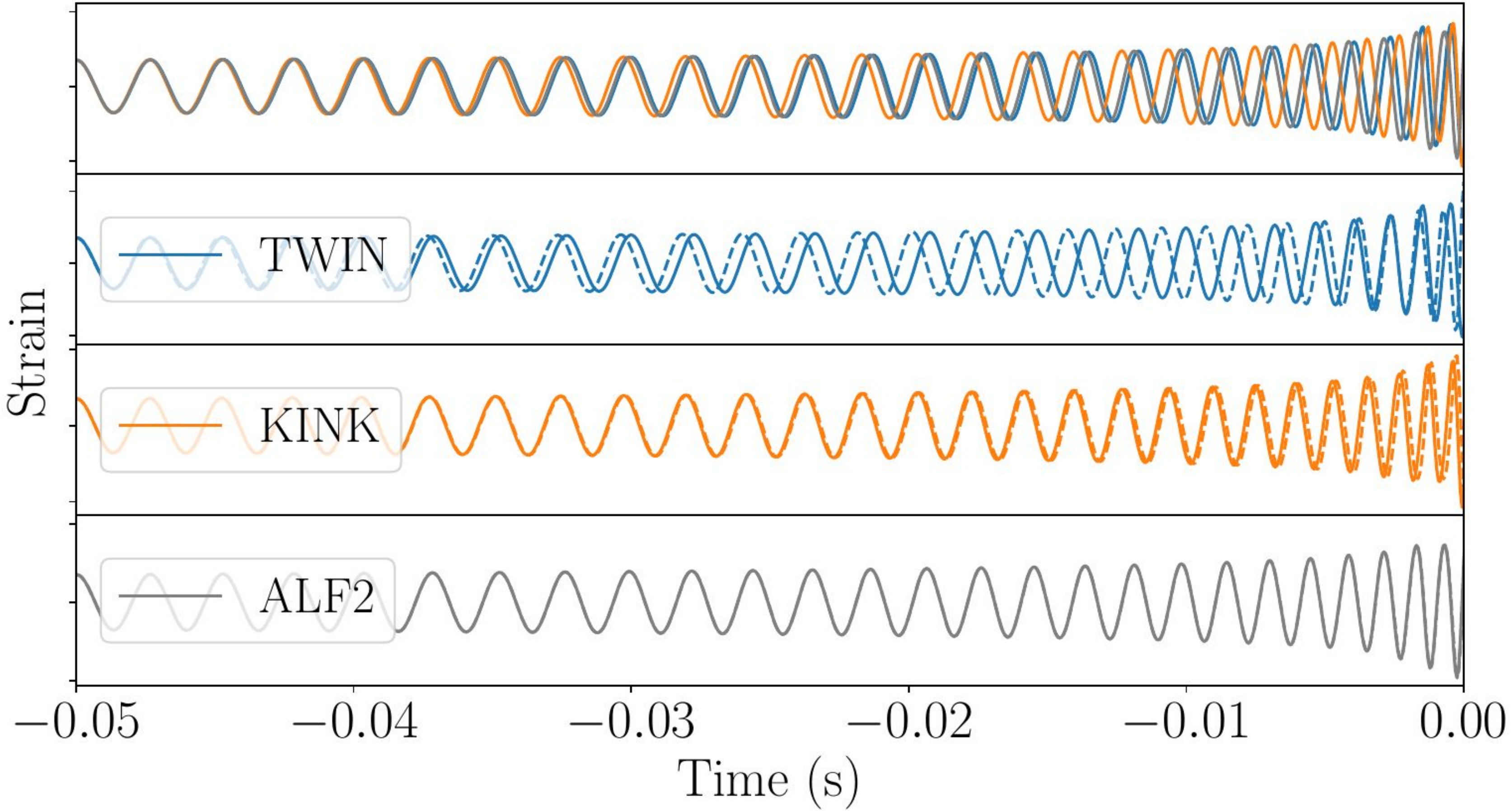
TWIN
KINK
ALF2
Strain
−0.05
−0.04
−0.03
−0.02
−0.01
0.00
Time (s)

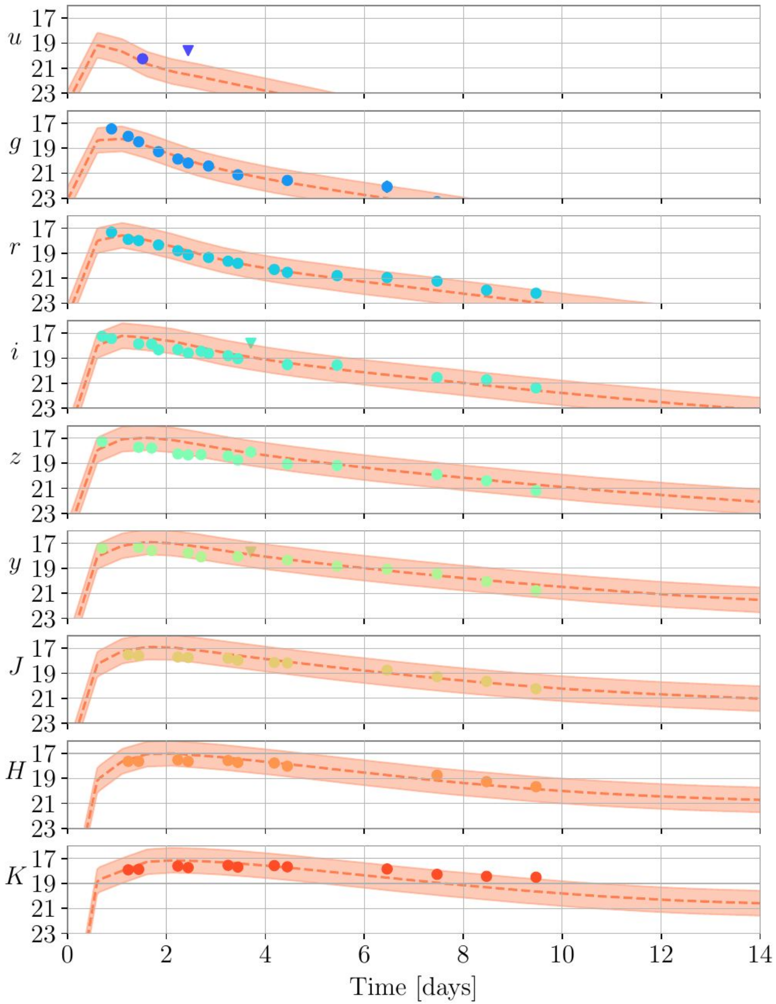
u
g
r
i
z
y
J
H
K
17
19
21
23
0
2
4
6
8
10
12
14
Time [days]

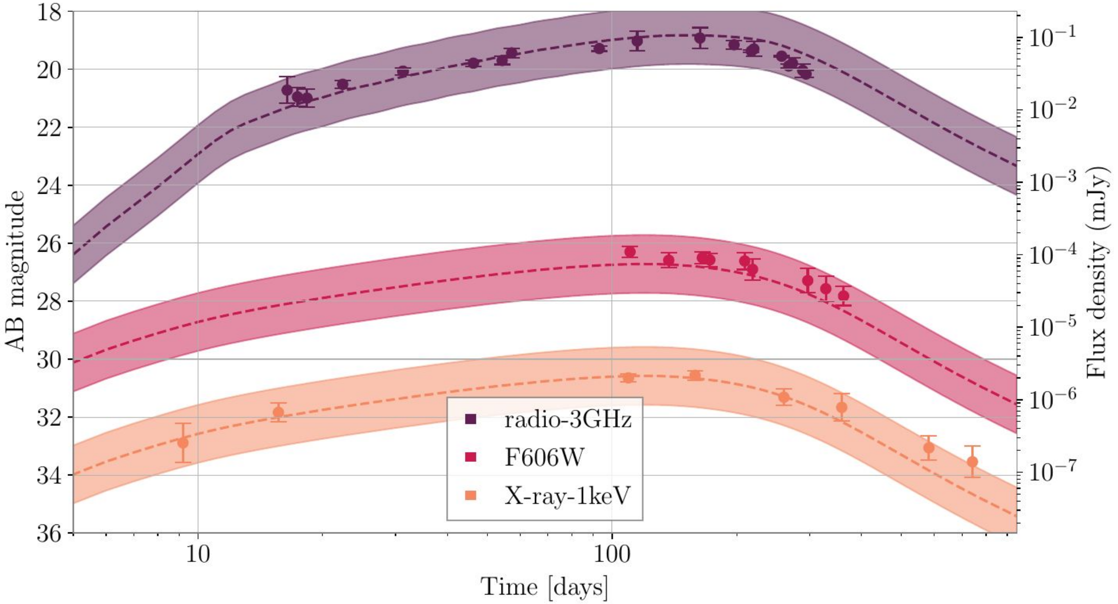
AB magnitude
Flux density (mJy)
Time [days]
radio-3GHz
F606W
X-ray-1keV
18
20
22
24
26
28
30
32
34
36
10
100
$10^{-1}$
$10^{-2}$
$10^{-3}$
$10^{-4}$
$10^{-5}$
$10^{-6}$
$10^{-7}$

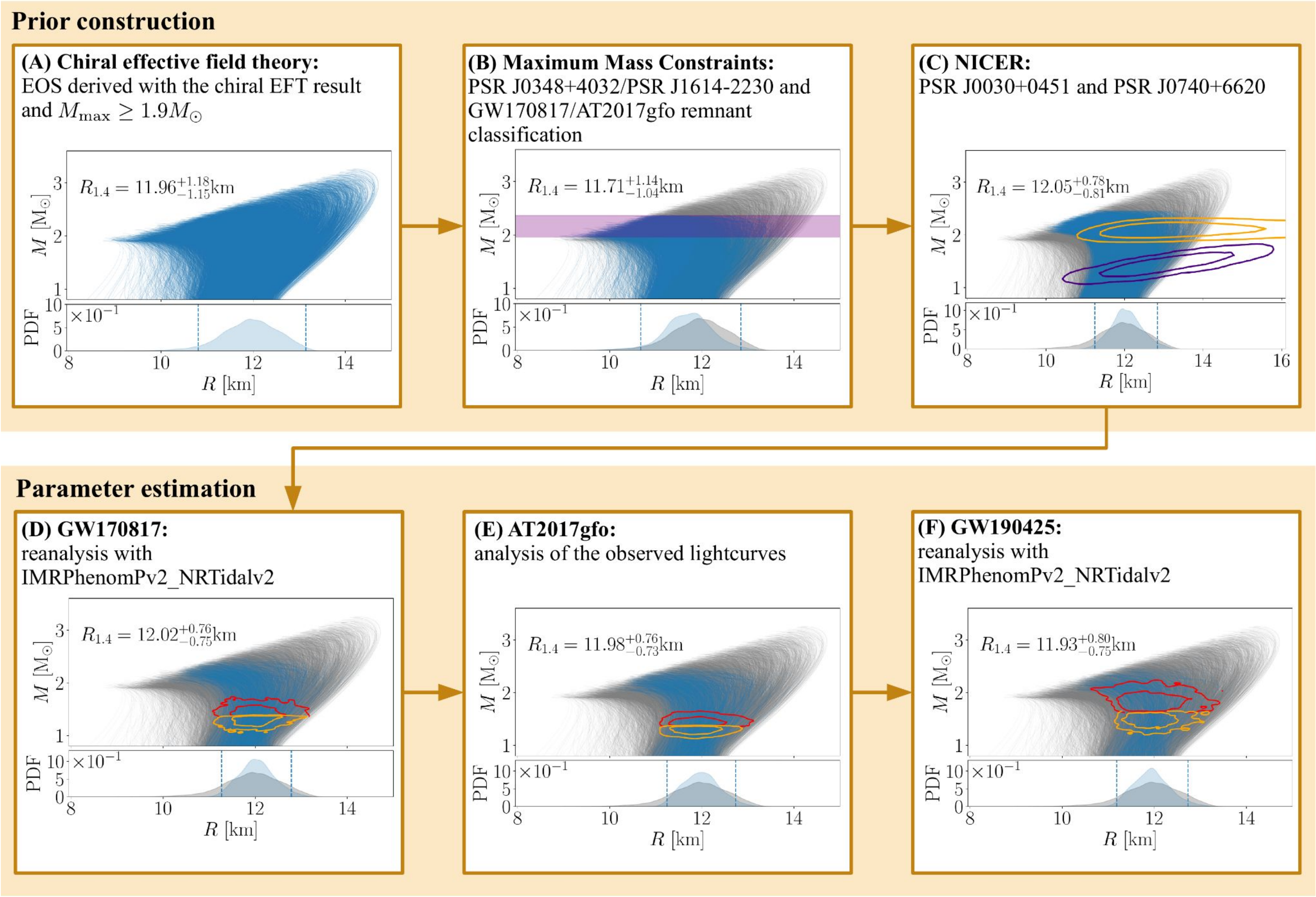

Prior construction
(A) Chiral effective field theory:
EOS derived with the chiral EFT result and $M_{\max} \geq 1.9 M_\odot$
$R_{1.4} = 11.96^{+1.18}_{-1.15}$km
(B) Maximum Mass Constraints:
PSR J0348+4032/PSR J1614-2230 and GW170817/AT2017gfo remnant classification
$R_{1.4} = 11.71^{+1.14}_{-1.04}$km
(C) NICER:
PSR J0030+0451 and PSR J0740+6620
$R_{1.4} = 12.05^{+0.78}_{-0.81}$km
Parameter estimation
(D) GW170817:
reanalysis with IMRPhenomPv2_NRTidalv2
$R_{1.4} = 12.02^{+0.76}_{-0.75}$km
(E) AT2017gfo:
analysis of the observed lightcurves
$R_{1.4} = 11.98^{+0.76}_{-0.73}$km
(F) GW190425:
reanalysis with IMRPhenomPv2_NRTidalv2
$R_{1.4} = 11.93^{+0.80}_{-0.75}$km
$M$ [M$_\odot$]
PDF
$\times 10^{-1}$
$R$ [km]

# Combing information

$$
\begin{aligned}
\mathcal{L}_{\mathrm{HIC}}(\mathrm{EOS}) &= \int dn\, dP\, p(\mathrm{HIC}|n, P)p(n, P|\mathrm{EOS}) \\
&\propto \int dn\, dP\, p(n, P|\mathrm{HIC})p(n, P|\mathrm{EOS}) \\
&\propto \int dn\, dP\, p(n, P|\mathrm{HIC})\delta(P - P(n, \mathbf{EOS})) \\
&= \int dn\, P(n, P = P(n; \mathbf{EOS})|\mathrm{HIC}) \,,
\end{aligned}
$$

# Result

| Density | Astro-only | HIC-only | Combined |
|---|---|---|---|
| $1.0\ n_{\text{sat}}$ | $2.00^{+0.52}_{-0.49}$ | $2.05^{+0.49}_{-0.45}$ | $2.11^{+0.49}_{-0.52}$ |
| $1.5\ n_{\text{sat}}$ | $5.84^{+1.96}_{-2.26}$ | $6.06^{+1.85}_{-2.04}$ | $6.25^{+1.90}_{-2.26}$ |
| $2.0\ n_{\text{sat}}$ | $18.44^{+16.24}_{-9.69}$ | $19.47^{+33.63}_{-11.67}$ | $19.07^{+15.27}_{-10.53}$ |
| $2.5\ n_{\text{sat}}$ | $45.05^{+39.80}_{-19.62}$ | $47.78^{+75.96}_{-32.96}$ | $45.43^{+40.41}_{-19.11}$ |

# Result

| Mass | Astro-only | HIC-only | Combined |
|---|---|---|---|
| $1.0M_{\odot}$ | $11.76^{+0.65}_{-0.71}$ | $11.89^{+0.79}_{-0.98}$ | $11.88^{+0.57}_{-0.76}$ |
| $1.4M_{\odot}$ | $11.94^{+0.79}_{-0.78}$ | $12.06^{+1.13}_{-1.18}$ | $12.01^{+0.78}_{-0.77}$ |
| $1.6M_{\odot}$ | $11.97^{+0.87}_{-0.78}$ | $12.11^{+1.33}_{-1.33}$ | $12.03^{+0.98}_{-0.75}$ |
| $2.0M_{\odot}$ | $11.88^{+1.23}_{-1.10}$ | $12.19^{+1.71}_{-1.59}$ | $11.91^{+1.24}_{-1.11}$ |